Smart Agricultural Technology 14 (2026) 102147

Contents lists available at ScienceDirect

Smart Agricultural Technology

journal homepage: www.journals.elsevier.com/smart-agricultural-technology

Technical validation of the Predictive Optimal Water and Energy Irrigation (POWEIr) controller for solar-powered drip irrigation

Carolyn Sheline[a,b,1], Fiona Grant[a,b,1,*], Georgia van de Zande[a,b], Shane Pratt[a,b], Samer Talozi[c], Ammar Namarneh[d], Anas Mansouri[e], Ahmed Wifaya[f], Vinay Nangia[e], Susan Amrose[a,b], Amos G. Winter V[a,b]

[a] Massachusetts Institute of Technology (MIT), USA
[b] K. Lisa Yang Global Engineering and Research (GEAR) Center, USA
[c] Civil Engineering Department, Jordan University of Science and Technology, Irbid, 22110, Jordan
[d] Methods for Irrigation and Agriculture (MIRRA), Amman, Jordan
[e] International Center for Agricultural Research in the Dry Areas (ICARDA), Rabat, Morocco
[f] National Institute of Agricultural Research (INRA), Agadir, Morocco

ARTICLE INFO

Keywords:
Solar power
Drip irrigation
Precision irrigation
Machine learning
Model predictive control

ABSTRACT

To feed the growing population, agriculture production must be intensified using existing resources. Sustainable agriculture intensification is particularly important in low and middle income countries (LMICs), which disproportionately experience food insecurity. This study evaluates the performance of a precision irrigation controller for solar-powered drip irrigation (SPDI) under real-world operating conditions. SPDI has the potential to increase water use efficiency and reduce fossil fuel use for irrigation. Precision irrigation technology could lower SPDI operating costs and enable sustainable irrigation practices among farmers with varied expertise. Despite these benefits, the adoption of SPDI and precision irrigation is limited in LMICs due to high investment costs and system complexity. Previous work proposed the Predictive Optimal Water and Energy Irrigation (POWEIr) controller as a precision irrigation solution that could meet the needs of farmers in resource-constrained contexts. This study quantifies the POWEIr controller performance in terms of water and energy savings, irrigation reliability, and system cost. The controller reduced water and energy use compared to typical farmer practice by up to 44% and 43%, respectively, while maintaining crop yield over three growing seasons. The controller used solar power for irrigation, but relied on a buffer battery to execute irrigation schedules. A yield loss sensitivity analysis found that increasing the controller's use of solar energy by about 40% would have been sufficient to reliably irrigate with solar alone. These results suggest that the POWEIr controller could enable reliable, low-cost SPDI systems, and if adopted, could make sustainable irrigation practices more accessible to farmers in LMICs.

1. Introduction

In 2022, an estimated 2.4 billion people faced moderate to severe food insecurity, a substantial increase from 2015 when the UN Sustainable Development Goals (SDGs) were first introduced [1]. This trend deviates from the trajectory needed to achieve the second SDG: zero hunger by 2030. This reported severe food insecurity disproportionately affects low- and middle-income countries (LMICs). To improve global food security, crop production must be intensified without overtaxing the world's natural resources [2,3]. Currently, agricultural practices account for 70% of global freshwater withdrawals, and agri-food systems produce 30% of global greenhouse gas emissions [4–7]. Improving water use efficiency is especially important in water-stressed regions like the Middle East and North Africa (MENA) [8].

Solar-powered drip irrigation (SPDI) has the potential to both conserve water and reduce fossil fuel use. Solar-powered water pumps are estimated to have 95%–98% lower total lifetime greenhouse gas emissions than pumps powered by grid electricity or diesel fuel [9]. The use of solar-powered irrigation pumps is growing rapidly in LMICs [10]. India, which contains the world's largest irrigated land area [11], has

* Corresponding author.
E-mail addresses: csheline@alum.mit.edu (C. Sheline), frgrant@alum.mit.edu (F. Grant), gdvdz@mit.edu (G. van de Zande), srpratt@mit.edu (S. Pratt), samerbse@just.edu.jo (S. Talozi), ammar-namarneh@mirra-jo.org (A. Namarneh), v.nangia@cgiar.org (V. Nangia), samrose@mit.edu (S. Amrose), awinter@mit.edu (A.G. Winter V).
[1] Co-lead authors, contributed equally to this work.

https://doi.org/10.1016/j.atech.2026.102147
Received 17 February 2026; Received in revised form 20 April 2026; Accepted 21 April 2026
Available online 22 April 2026

Nomenclature

POWEIr	Predictive Optimal Water and Energy Irrigation
LMIC	Low and middle income country
SPDI	Solar-powered drip irrigation
SDG	Sustainable Development Goal
MENA	Middle East and North Africa
MPC	Model predictive control
SPM	Solar profile matching
SSO	Single section operation
PSF	Percent solar fill
VAR	Vector auto-regression
TMY	Typical meteorological year
LSTM	Long short-term memory
MQTT	Message queuing telemetry transport
VFD	Variable frequency drive
EC	Electrical conductivity
WUE	Water use efficiency
LFP	Lithium iron phosphate
DAQ	Data acquisition unit

installed over 2.1 million solar irrigation pumps since 2019 through government subsidies [12,13]. In Sub-Saharan Africa, the uptake of solar pumps is also expanding with the aim of increasing irrigated agriculture and alleviating poverty [10]. Drip irrigation delivers water to the crop root zone through a network of pipes and emitters. When operated properly, drip irrigation is estimated to decrease water use by 40% and increase crop yields by 20% compared to traditional flood and furrow irrigation methods [14,15]. In addition, precision irrigation technologies, which aim to calculate and deliver precise amounts of water and nutrients to the crop, can help farmers to manage complex irrigation decisions [16] and improve resource use efficiency at the farm level [17]. Precision irrigation control can also reduce SPDI operating costs [18–20], which could make sustainable irrigation practices more accessible to resource-constrained farmers.

Despite the potential benefits and policy incentives, farmers in LMICs still face barriers to adopting SPDI and precision irrigation technology. These barriers include high investment cost, increased system complexity, lack of technical support, and farmers' risk aversion [21–23]. Although drip irrigation alone has been more widely adopted, farmers often operate the system unsustainably—over-irrigating and wasting energy—due to a lack of knowledge or a desire to mitigate risk to their crops and livelihoods [24–26]. Existing precision irrigation controllers use integrated sensors to monitor the crop, soil, weather conditions, and system performance to make decisions about irrigation scheduling [27]. These control systems can cost tens of thousands of dollars (USD) [28], and require on-site network connectivity, access to specialized hardware, and expert fine-tuning of the control algorithm [29,30]. The high price point and operational complexity of these technologies make them inaccessible to many LMIC farmers [17]. There is a need for a low-cost precision irrigation controller that is designed for the LMIC context to facilitate farmers' adoption of sustainable irrigation practices, such as SPDI. To make an impact in resource-constrained markets, the controller must be scale-neutral, adaptable to a variety of use cases, affordable, and technologically accessible to farmers with a wide range of expertise [31].

Although precision irrigation control is an active area of research, there are few solutions that seek to address the specific needs and constraints of LMIC farmers [23,32]. In the literature, precision irrigation solutions leverage Internet of Things (IoT) sensor platforms, machine learning, artificial intelligence (AI), cloud-based computing, and a variety of optimization techniques [30]. Previous studies have demonstrated water savings of 11%–72% and crop yield increases of 15%–40% when comparing precision irrigation solutions to traditional irrigation practices [23,30]. However, recent systematic literature reviews have identified several barriers to the scalability of these solutions, particularly in resource-constrained contexts. IoT platforms that rely on full-field sensor suits are limited by complex installation and calibration requirements as well as high maintenance costs [30,33]. Systems that rely on cloud-based computing for data processing, predictive modeling, and optimization can be limited by high computational costs and the need for robust on-site connectivity [32,33]. Previous research has primarily focused on simulation-based analysis or small-scale pilots, so there is a lack of long-term, field-scale testing of the proposed solutions [30,32]. Literature reviews highlight the need to balance farmer expertise with potentially expensive data-driven control systems to develop precision agriculture technologies that are scalable and well-suited to LMIC contexts [23,30,34].

In a prior study, the authors introduced the Predictive Optimal Water and Energy Irrigation (POWEIr) controller for SPDI, a solution designed to make sustainable irrigation practices technologically and economically accessible to resource-constrained farmers [18]. The POWEIr controller employs model predictive control (MPC) to co-optimize SPDI water and energy use and only requires a low-cost weather station and a pressure sensor for feedback. The controller produces optimal irrigation schedules specific to a given use case and communicates the schedule directly to the farmer. The controller is intentionally designed to use a limited number of sensors to make the device less expensive than existing solutions that use full-field sensor suites [27]. The authors previously explored the impact of using low-cost, lower accuracy weather sensors for the controller's irrigation demand prediction and found minimal impact on crop yield in simulation [35].

Recent work has demonstrated that MPC, a process control technique, is more suitable for irrigation systems than classical feedback, rule-based, or fuzzy-logic controllers, methods which often require detailed inputs and on-site fine tuning [34,36,37]. MPC uses a dynamic model to predict system behavior over a moving time window and optimize system performance based on an objective function, a set of constraints, and real-time measurements [34]. Because the dynamic model is inherently specific to the system being controlled, the MPC approach is scale-neutral and can adapt to variable weather conditions and crop behavior during SPDI operation.

Previous studies have demonstrated that MPC-based irrigation controllers can reduce water use while avoiding crop stress [38] and can lower water consumption compared to other irrigation control techniques [36,39–41]. These studies focus on water use optimization, but do not examine irrigation scheduling with solar power or energy use optimization. Prior work finds that an irrigation controller must manage both energy and water use efficiency to realize the economic benefits of solar-powered irrigation at the farm level [20,23]. In addition to optimizing for minimal water use, the POWEIr controller implements solar profile matching (SPM) schedules. SPM involves scheduling irrigation events such that the pump operating power closely matches the available solar power profile throughout the day by varying the number of open field sections (Fig. 1). SPM ensures more efficient use of the available solar energy, minimizing the use of an alternate power source such as a battery or grid connection, and thereby lowers the power system cost compared to the current practice of single section operation (SSO) [18,42,43].

The POWEIr controller concept was initially demonstrated with a small-scale prototype and simulated SPDI system operation [18]. The study found that the optimized SPM schedule increased the irrigation delivered directly by solar by 19%–46% and decreased the required battery capacity by 78%–98% compared to the typical SSO schedule used by farmers. In a separate study, Sheline et al. [35] evaluated the impact of using a low-cost weather station compared to state-of-the-art sensors on the POWEIr irrigation schedule and simulated crop yield. The study found that the low-cost sensors led to a 15% decrease in total scheduled irrigation, but this change had negligible effect on the simulated crop yield. Although previous work showed promising initial results, the POWEIr controller performance must be validated at scale, over longer

periods, and under a variety of operating conditions to ensure that the simulated benefits will translate to real-world outcomes. The scheduling uncertainty introduced by the proposed controller has yet to be characterized, which means the irrigation reliability of the SPDI-SPM system is unknown. Quantifying the controller's performance under real-world operating conditions will help facilitate the design of low-cost, reliable SPDI systems.

In a companion study, the authors conducted a needs assessment for precision irrigation control in resource-constrained markets with farmers, expert professionals, and industry stakeholders [16]. The study identified the functional requirements and associated design target specifications for a controller that could be valuable and accessible to farmers in LMICs. Functional requirements describe the functions a device must perform to fulfill the needs of the intended end-user [44,45]. Target specifications are the performance metrics the device must meet to produce the desired functional outcomes [45]. Functional requirements and target specifications are defined in the preliminary design stage and refined through literature and prior art review, stakeholder interactions, and prototype testing.

The needs assessment study identified the controller functional requirements and target specifications through a combination of irrigation market stakeholder interviews, farmer focus groups, and the precision irrigation control literature. Broadly, the study found that farmers were particularly interested in precision irrigation as a means to mitigate risk to their crops and assist irrigation decision-making. Both farmers and industry professionals emphasized the novelty of a controller that optimizes both water and energy use concurrently, and observed that this could enable more affordable solar power systems for farmers. The study suggests that the POWEIr controller should be designed to meet the following target specifications:

- Increase water and energy use efficiency relative to drip irrigation operated with current farmer practices and decision-making, specifically
  - a 10%–50% reduction in the farmer's water use, which would be comparable to the performance of existing precision irrigation controllers with full-field sensor suites;
  - a 10% increase in energy use efficiency compared to current irrigation scheduling practices (SSO) to lower the cost of solar power systems for irrigation;
- Accurately compute irrigation volume within 10% of crop water demand to mitigate risk to crop yield;
- Ensure reliable operation such that power is always available for scheduled irrigation events.

Furthermore, the study identified the need to keep the user in the control loop, allowing farmers to adjust the irrigation schedule to mitigate risk and build trust in the device. Finally, the controller must be able to function with manual or automatic valves to accommodate the variety in farmer technical expertise and equipment accessibility.

The present study quantifies the performance of the proposed POWEIr controller on farms in the MENA region and analyzes sources of irrigation scheduling uncertainty introduced by the controller. The controller's performance is then validated against the above target specifications from the previous needs assessment study [16]. The experiments were conducted in Jordan and Morocco, two countries that are invested in promoting sustainable irrigation practices and renewable energy use in agriculture [46,47]. Finally, a yield loss sensitivity analysis was conducted in simulation to determine the controller's impact on SPDI-SPM irrigation reliability and power system cost.

The research aims of this paper are to:

1. Demonstrate the full-scale implementation of the POWEIr controller in multiple contexts;
2. Validate the controller's performance in terms of water use, energy consumption, and irrigation reliability against the identified target specifications;
3. Quantify the impact of the controller's scheduling uncertainty on crop yield and power system cost;
4. Propose refinements to the POWEIr controller design.

Based on the literature and previous work, the POWEIr controller has the potential to make the benefits of precision irrigation affordable and accessible to resource-constrained farmers. By demonstrating the controller's performance under real-world operating conditions, this study aims to expand the target market for precision agriculture technology and increase the use of sustainable irrigation practices.

2. POWEIr controller theory and design

This section summarizes the POWEIr controller theory and provides a fundamental understanding of its control levels and physical models. A full description of the theory is reported in Sheline et al. [18], with updates to the solar power prediction model reported in Sheline et al. [35].

Fig. 1 depicts the POWEIr controller architecture, which consists of two control levels:

- **Level S** uses machine learning to forecast daily weather and uses MPC to optimize the irrigation schedule,
- **Level P** controls the pump operating point to facilitate multi-section operation for the SPM schedules.

In the MPC algorithm, the process being controlled is irrigation, and the dynamic model captures the behavior of the SPDI system, which includes the local weather, agronomy, pump, and solar power system. Level S produces SPM schedules, which means the pump operating points for single and multiple sections must be known. Level P uses pressure feedback control to ensure that the pump provides sufficient pressure for uniform emitter flow without over-pressurizing the hydraulic system and wasting energy. A one-time calibration must be conducted to obtain the pressure setpoint for various section permutations. The controller hardware includes a low-cost weather station for Level S and a pressure sensor for Level P. The predictive modeling and optimization are conducted via cloud computing to reduce the need for specialized on-site hardware. These hardware choices, which informed the software design, aim to make the controller simple to maintain and affordable to the target users.

Level S takes in measured and historical weather data as well as use case parameters, including crop(s), soil type(s), field layout, GPS coordinates, power system and pump technical specifications, and the pump operating points. An engineer would measure and program these parameters into the controller during its initial installation and calibration. Level S forecasts daily weather and uses a soil moisture model to predict crop water demand for the day. Based on the water demand and predicted solar power profile, Level S produces an optimized irrigation schedule at the beginning of the day that the controller communicates to the farmer. The needs assessment conducted by Van de Zande et al. [16] found that farmers preferred a daily irrigation schedule, but the Level S algorithm can accommodate different prediction time windows. The controller monitors the irrigation delivered based on the duration each section is open, either through automatic valves or through the farmer confirming manual valve operation via the user interface (smartphone app [48]). In this way, the controller also keeps track of changes the farmer makes to the irrigation schedule. During operation, Level P maintains the pump operating pressure setpoint for the current section configuration.

2.1. Level S: Irrigation schedule optimization

2.1.1. Objective function and constraints

The Level S optimization minimizes water use, maximizes solar energy use through SPM, and minimizes risk to the crop yield. The objective function, expressed in units of cost, is formulated as

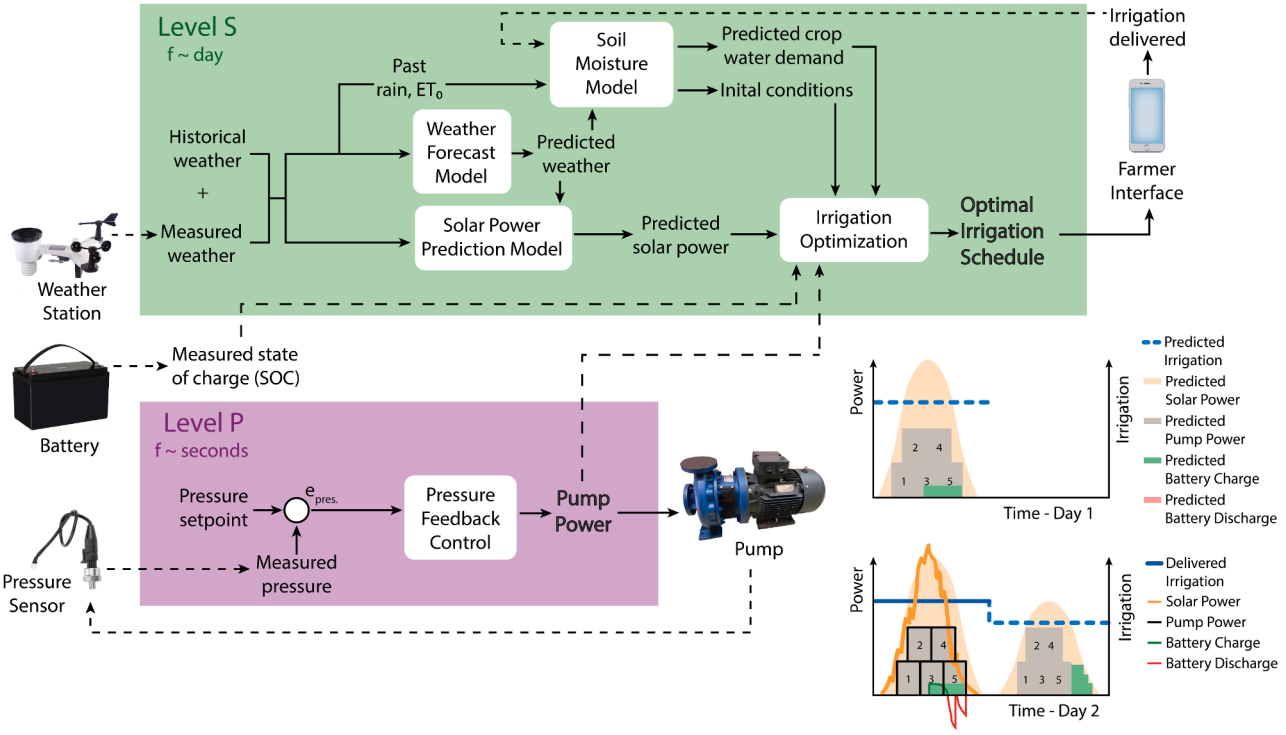

Fig. 1. The Predictive Optimal Water and Energy Irrigation (POWEIr) controller architecture. At the start of the day Level S (green) optimizes an irrigation schedule based on measured and historical weather data. These data are used to train the weather forecast model and initialize the soil moisture model. The future solar power profile and weather parameters, including reference evapotranspiration (ET_0) and precipitation are predicted. The soil moisture model takes in these parameters to calculate crop water demand. The optimized irrigation schedule for the upcoming day is communicated to the farmer through a smartphone app. The measured irrigation delivered during the day is fed back into Level S, keeping the farmer in the control loop. Level P (purple) maintains calibrated pump operating points using pressure feedback control, facilitating solar profile matching (SPM) operation. The bottom right plots illustrate SPDI system operation, utilizing SPM, with the controller over a 24-hour period. (For interpretation of the references to colour in this figure legend, the reader is referred to the web version of this article.)

$$min\left[\sum_{i=\delta t}^{N_{hor}}\frac{1}{N_{hor}}\left(k_b u_{max}(u_{1,i}-u_{2,i})+\sum_{s=1}^{N_{s,tot}}k_w q_s d_{s,i}\right)-\sum_{n=1}^{N_{day}}\sum_{s=1}^{N_{s,tot}}\frac{1}{N_{day}}\left(k_c A_s\frac{dY_{a,s,n}}{dt}\right)+k_d(1-SOC_{N_{hor}})\right], \quad (1)$$

where N_{hor} and N_{day} are the MPC prediction horizon in hours and days, δt is the hourly time step, and $N_{s,tot}$ is the total number of field sections. The first term of the objective minimizes battery use, prioritizing the use of solar power for irrigation and thus SPM, and minimizes the irrigation volume delivered over the prediction horizon to reduce water use. Here, k_b is the unit cost of the battery in USD/kWh; $u_{\max}$ is the maximum battery dispatch rate in kW recommended by the manufacturer to prevent battery aging; u_1 and u_2 are the battery charging and discharging rate, respectively, as a fraction of the allowed maximum dispatch rate; k_w is the unit cost of water in USD/m^3; q_s is the section flow rate in m^3/h; and d_s is the binary valve state (open/closed) for section s. The second term of the objective ensures the crop water demand is met by maximizing the estimated crop yield, which is a function of irrigation volume. Here, k_c is the crop price in USD/kg and A_s is the section area in m^2. The daily change in crop yield, $\frac{dY_{a,s,n}}{dt}$, is estimated as the yield, Y_a in kg/m^2, divided by the number of days in the crop growing season. The yield calculation is described later in this section. The final term of the objective ensures the battery is charged with any excess solar energy by the end of the prediction horizon such that the battery buffer is ready for the next day. The buffer is a fail-safe if solar power is unavailable for an irrigation event due to Level S prediction error. Here, k_d in USD/day is the daily cost of the battery based on its lifetime cost, and SOC is the battery state of charge.

The output of the Level S optimization is the irrigation schedule expressed as the time and duration of irrigation for each field section throughout the day. The control variables, u_1, u_2, d_s, and SOC are subject to physical bounds:

$$0 \le u_{1,i} \le 1, \quad (2)$$

$$-1 \le u_{2,i} \le 0, \quad (3)$$

$$d_{s,i} \in \{1,0\}, \quad (4)$$

$$SOC_{min} \le SOC_i \le SOC_{max}, \quad (5)$$

where $SOC_{\min}$ is the maximum depth of discharge recommended by the manufacturer, and $SOC_{\max}$ is the maximum state of charge, typically 1. In addition, the battery is only allowed to charge when surplus solar power is available and discharge when the pump power exceeds the available solar power; these constraints prioritize the use of solar power for irrigation. A full description of constraints and initial conditions is provided in Appendix A.1. The remainder of this section describes the physical models used to calculate the parameters and variables in the Level S objective function.

2.1.2. Weather forecast model

Weather data are needed to predict the daily crop water demand and available solar power. Level S employs a machine learning algorithm to forecast solar irradiance, precipitation, air temperature, relative humidity, and wind speed. These data are passed into a soil moisture model and solar power model to make the predictions. The on-site, low-cost weather station is necessary for use cases in LMICs where accurate local weather forecasts are not readily available [49,50], or in rural settings

where the nearest weather station may be thousands of kilometers away [51,52].

The selected machine learning algorithm is vector autoregression (VAR). The VAR algorithm makes multiple variable time-series predictions from related variables. This algorithm is well-suited for resource-constrained settings as it is computationally inexpensive and does not require large amounts of training data [53]. Daily average, minimum, and maximum air temperature and relative humidity, average wind speed, total solar radiation, total sun hours (calculated as the number of hours the hourly radiation is greater than 0.1 MJ/m^2), the reference evapotranspiration (which is used to estimate crop water demand), and total precipitation are the data variables used in the VAR algorithm. The VAR model receives a defined time window of input data and forecasts a vector of the same data for the upcoming prediction period. The VAR algorithm is trained using a combination of one year of typical meteorological year (TMY) data obtained from the nearest weather station and previous measurements from the on-site weather station. To maintain accuracy, the VAR algorithm undergoes periodic retraining and reconstruction using both historical and incoming weather data at the beginning of each prediction cycle. This process ensures that the algorithm captures and adapts to current trends in the data.

2.1.3. Soil moisture model and crop yield estimate

The soil moisture model estimates the daily crop water demand, which is an input to the irrigation schedule optimization. The model uses the predicted daily weather parameters, namely precipitation, Pr, and crop evapotranspiration, ET_c. The ET_c is calculated as

$$ET_c = K_c ET_0, \tag{6}$$

where ET_0 is the reference evapotranspiration in mm and K_c is the crop coefficient. The weather forecast model takes in Pr and ET_0 values calculated for previous days to predict the Pr and ET_0 for the soil moisture calculations. The POWEIr controller uses the Penman-Monteith equation described in [54] to calculate ET_0. The Penman-Monteith equation assumes a grass reference crop of 0.12 m height with complete ground shading and sufficient soil moisture. Under these assumptions, ET_0 depends solely on air temperature, relative humidity, solar irradiance, and wind speed. These weather data inputs, along with Pr, are measured with a local weather station and tabulated to get daily averages and totals.

The soil moisture model conducts a soil water balance, which tracks the inflow, outflow, and retention of water within the soil. These values are calculated every day throughout the growing season, which is defined by the crop planting and harvesting dates. The soil water balance, defined in [54], is

$$D_{r,n} + (1 - k_{RO}) Pr_n + \frac{1000 I_{del,n}}{A_s f_w} = D_{r,n-1} + K_{st} ET_{c,n}, \tag{7}$$

where $D_{r,n}$ is the root zone depletion in mm on day n, k_{RO} is the runoff coefficient based on the soil texture, I_{del} is the delivered irrigation volume in m^3, A_s is section area in m^2, f_w is the soil wetted fraction, and K_{st} is the crop water stress coefficient. K_{st} is calculated as

$$K_{st} = \frac{TAW - D_r}{TAW(1 - f_d)}, \tag{8}$$

where f_d is depletion fraction, which is calculated as

$$f_{d,n} = f_{d,const} + 0.04(5 - ET_{c,n}). \tag{9}$$

The $f_{d,const}$ is a crop-dependent constant defined in [54]. TAW is the total available water that the crop can extract from the soil in mm, and it depends on the crop root depth, Z_r in m, and the soil texture.

The soil moisture is equated to the volumetric soil water content, θ_v, which is defined as

$$\theta_v = \frac{V_{water}}{V_{soil}}, \tag{10}$$

where V_{water} is the volume of water in the soil in m^3, and V_{soil} is the soil volume in m^3. The θ_v in the root zone can be related to D_r as

$$\theta_{v,n} = \theta_{v,fc} - \frac{D_{r,n}}{1000 Z_r}, \tag{11}$$

where $\theta_{v,fc}$ is the volumetric soil water content at field capacity and depends on the soil texture. D_r is constrained to be less than TAW and greater than zero. If D_r is greater than the readily available water, RAW, which is defined as

$$RAW_n = f_{d,n} TAW, \tag{12}$$

the crop experiences water stress and K_{st} is between zero and one. If D_r is less than or equal to RAW, the crop is not water stressed and K_{st} is one.

The water stress affects the crop evapotranspiration rate, which is adjusted as

$$ET_{c,adj} = K_{st} ET_c. \tag{13}$$

Here, $ET_{c,adj}$ is the actual crop evapotranspiration. When the crop experiences water stress, K_{st} is less than one and the reduction in evapotranspiration leads to a reduction in yield. The adjusted crop yield, Y_a, is calculated as

$$1 - \frac{Y_a}{Y_{max}} = K_y \left(1 - \frac{ET_{c,adj}}{ET_c}\right), \tag{14}$$

where K_y is the crop yield response factor [55], and $Y_{\max}$ is the maximum possible yield in kg/m^2. $Y_{\max}$ is determined using the agro-ecological zone method defined in [56].

2.1.4. Solar power prediction model

The power output of the solar panels is estimated using a single-diode model. The single-diode model was selected based on its demonstrated simplicity and accuracy in estimating maximum panel power output under varying weather conditions [57]. The model takes in hourly solar irradiance and temperature data along with the panel specifications provided by the manufacturer. The additional parameters used in the single-diode model are computed using the methodology outlined in [58].

To predict the daily solar power curve, the weather forecast model takes in solar power measured by the controller on previous days and TMY weather data and employs a Long Short-Term Memory (LSTM) network [59]. An LSTM network is a type of recurrent neural network notable for its ability to retain past information, resistance to noise, and suitability for sequence data prediction. The choice of an LSTM network is informed by its aptitude for single-variable time series prediction over a full day's solar profile [60,61].

The LSTM algorithm was developed using the Keras deep learning package [62]. The architecture of the LSTM model comprises a 100-cell LSTM layer with ReLU activation, a 50-cell LSTM layer with ReLU activation, and a dense layer [59]. The loss function employed is a mean square error, and the optimization algorithm used is Adam [63]. The LSTM algorithm is trained using one year of TMY data obtained from the nearest weather station, combined with measured data from the on-site weather station. Periodic retraining and reconstruction of the LSTM model occur at the start of each prediction cycle, ensuring that the algorithm incorporates all current data trends.

2.2. Level P: Pump operating point control

Level P maintains the pump operating point using proportional-integral control on the pump pressure with a single feedback pressure sensor. Pressure feedback control is well-suited for SPDI systems as drip emitters have a minimum operating pressure at which they uniformly produce their rated flow [64]; this control technique maintains the minimum pressure necessary to operate the emitters without wasting power by over-pressurizing the hydraulic system.

The feedback pressure sensor is placed downstream of the pump, filters, and fertigation unit, which mixes fertilizer into the irrigation water. Previous experimental work observed that, due to clogging, the filter and fertigation unit are the primary dynamic pressure losses in the hydraulic system [65,66]. Placing the feedback sensor downstream of these components in the main pipe ensures that the pump operating point can be calibrated once with static pressure set points for the field section configurations. The controller is programmed with the calibrated pump operating power for single and multiple sections, and these operating points are passed into the Level S optimization. Although the pump power will vary over time, Level P ensures that the pump operating points are relatively consistent, barring any significant changes that would require hydraulic maintenance. This means Level P facilitates accurate predictive modeling in Level S over the irrigation season.

3. POWEIr controller validation methods

The POWEIr controller validation was conducted in two parts: experiment and simulation. A controller prototype was installed on farms in Jordan and Morocco to measure water use, energy consumption, and crop yield. The controller's performance was compared to a reference drip system operated with local farmers' practices. As the experiment fields were small with short daily irrigation times (4.5 h/day in Jordan, 6 h/day in Morocco), the systems were designed to operate with direct drive solar power (i.e., no battery). A buffer battery was included to prevent failed irrigation events while testing how effectively Level S maximized solar energy use for irrigation. A yield loss sensitivity analysis was conducted in simulation to characterize the controller's irrigation reliability with a direct drive solar power system. The impact of the controller's reliability on power system cost was examined, and improvements to the controller software were proposed. The power system component costs were based on the equipment prices collected from local vendors.

The controller was validated against the target specifications identified by Van de Zande et al. [16], as summarized in the Introduction. The target specifications for resource use efficiency were 10%–50% water savings and a 10% increase in energy use efficiency compared to a typical farmer's drip system. The target for irrigation accuracy was to estimate crop water demand within ±10%. As shown in the soil moisture model (Section 2.1.3), the exact crop water demand depends on the root zone soil conditions, micro-climate, and crop parameters, which can vary across the field. This makes it difficult to obtain a ground truth value for the crop water demand. Instead, the controller's ability to accurately estimate soil moisture content was compared to on-field measurements, and the crop yield of the controller and reference fields were compared. A previous study validated the accuracy of the weather forecast model (Section 2.1.2) in predicting the parameters for the crop water demand calculation [35].

3.1. Experimental methods

The controller validation experiment was used to measure the performance of the POWEIr controller across multiple farm contexts and identify sources of Level S scheduling error. Total water and pump energy use were measured on fields with the POWEIr controller and compared to similar fields irrigated based on farmers' typical practices for each location and crop type. The total cumulative pump energy and irrigation amount, I_{total} in m^3/ha, used by the POWEIr controller as well as the total crop yield, Y_{total} in tonne/ha, were compared to the reference field as indicators of performance. The reference fields were irrigated conventionally based on local practices. The water use efficiency, WUE in kg/m^3, was defined as

$$WUE = \frac{Y_{total}}{I_{total}} \times 1000. \tag{15}$$

The WUE was compared between the controller and reference fields. The accuracy of the soil moisture calculation was determined by comparing the Level S soil moisture estimates to soil moisture sensor data and in-field bulk soil measurements. The solar power predictions made by the controller were compared to the measured solar panel power output to calculate the Level S prediction error.

3.1.1. Field setup in Jordan and Morocco

Customized versions of the POWEIr controller were implemented in Jordan and Morocco, based on farmers' needs in each location identified in the previous stakeholder assessment study [16]. Both versions optimized the irrigation schedule using the theory presented in Section 2. In Jordan, the controller field was operated with manual valves and relied on the user to open and close field sections at the specified times, communicating via a custom phone app [48]. The app users in Jordan were farmhands and on-site researchers with expertise in irrigation management. The version tested in Morocco used automatic valves (Netafim Aquative Plus Actuator Valve) to operate the field sections, and the user monitored irrigation in the app. The app users in Morocco were on-site researchers. Fig. 2 shows the experimental setup, including the sensors, hydraulic system layout, valve operation, irrigation scheduling method, energy source, and crop type. Experiment site details are summarized in Appendix Table A.1.

In Jordan, the POWEIr controller was installed on a 1 ha research farm, operated by MIRRA[1], growing young grape vines and okra from May to December 2023. The grapes and okra were intercropped with separate sections and laterals. This means the effective controller and reference field areas were approximately 1 ha each. Half of the MIRRA research farm used the POWEIr controller to irrigate and the other half irrigated based on a local farmer's recommendations as a reference. The POWEIr controller field had an SPDI system with six sections where the grapes and okra could be irrigated separately. The reference field used grid power and drip irrigation with six sections where the grapes and okra could be irrigated separately. Both fields used manual valves. As young grape vines do not produce yield in the first season, only the okra crop yield was measured for the experiment.

In Morocco, the POWEIr controller was installed at the INRA[2] Agadir research site that grew potatoes from January to June 2023 and carrots from July to November 2023. The controller field of 0.6 ha was split into six sections. Due to the small field size and low daily water requirement, the system was able to irrigate the potato sections sequentially, and therefore, the controller only generated SSO schedules for the potato season. For the carrot season, a virtual farm with five times the actual area was simulated in the Level S optimization to ensure SPM schedules would be produced for the controller field. This means the effective experimental field area was 3 ha for the carrots. A small farm that sells to the local market was chosen as a reference for measuring typical irrigation practices. The reference field of 0.6 ha had an SPDI system and four sections with manual valves and grew the same crops at the same time as the controller field.

The experiment locations and crop types were selected based on the recommendations of the local research partners and previous studies that identified typical field sizes, crop types, and operating characteristics of farms in the target markets [16,67]. The research partners also ensured the reference fields employed irrigation practices that reflected farmers' typical irrigation practices. Irrigation practices were primarily based on farmer experience and field observations, including the crop growth stage and weather conditions. Water was typically applied in single irrigation events several times per week, with frequency and duration adjusted in response to the farmer's prior experience with the crop and the environmental conditions.

[1] Methods for Irrigation and Agriculture (MIRRA) is a private Jordanian non-profit research and development organization established in 2007.

[2] The National Institute of Agronomic Research (Institut National de la Recherche Agronomique) is a public research organization for agriculture in Morocco.

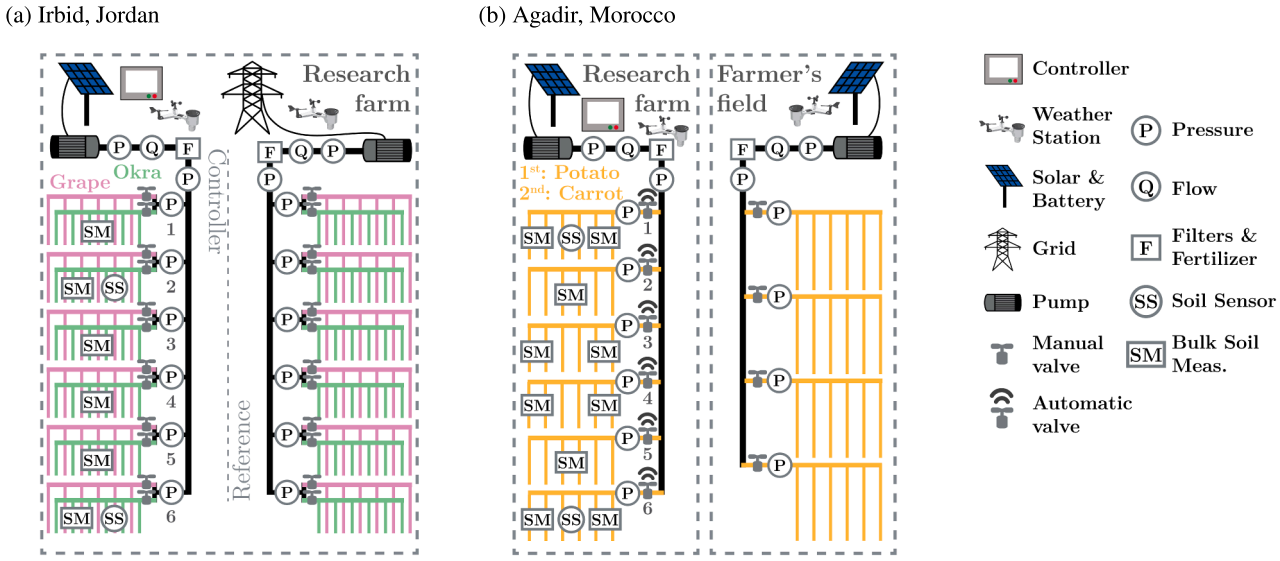

Fig. 2. The experimental setups in **a** Irbid, Jordan, and **b** Agadir, Morocco. In Jordan, a 1 ha research farm irrigated inter-cropped grapes and okra, with half of the farm using the POWEIr controller and solar power on six sections, and the other half irrigating based on a local farmer's recommendations with grid power as a reference. In Morocco, a 0.6 ha field at an INRA research site irrigated potatoes in the first season and carrots in the second season using the POWEIr controller and automatic valves on six sections compared to a neighboring farmer's 0.6 ha field with manual valves that irrigated the same crops in the same seasons based on the farmer's experience. Both of the experiments used drip irrigation and had weather stations, pressure sensors at the start of each section, a flow meter in the main pipe, a feedback pressure sensor after the pump, filters, and fertigation units.

Both sites experienced seasonally dry conditions characteristic of semi-arid climates. Irbid exhibited a Mediterranean rainfall regime with winter precipitation. Agadir was more consistently semi-arid with temperatures moderated by proximity to the Atlantic Ocean, yet was also subject to extreme heat events during the growing season.

3.1.2. Controller software and calibration

The POWEIr controller was programmed in Python. As described in Sheline et al. [18], a VAR algorithm was implemented using statsmodels (version 0.13.5; 2022) to predict daily weather. Additionally, as reported in Sheline et al. [35], an LSTM network was employed to predict the 24-hour solar power availability curve using the TensorFlow Keras API (version 2.11.0; 2022). The Level S code ran once per day in each country. At times when Level S was inactive for troubleshooting, on-site researchers used the FAO 56 [54] soil water balance method to estimate the crop water needs, similar to the method described in Section 2.1.3. The specific method used is noted when presenting data in Section 4. Node-RED [84] was used to program the sensors and hardware. An MQTT protocol was used to communicate the necessary input and output data between the different POWEIr controller levels, hardware, sensors, and the app. Data were stored in an InfluxDB [85] database that could be monitored remotely.

When evaluating the controller accuracy with the low-cost weather station, Sheline et al. [35] found that errors in crop parameter inputs, especially errors in the crop coefficients, significantly affected the irrigation volume and crop yield. Therefore, it was suggested that calibrated crop coefficients be used with the POWEIr controller for the full-scale experiments. Default agronomy parameters defined in [54] were used where applicable. The default parameters were adjusted in Jordan based on literature sources [68–71], and in Morocco based on the Ministry of Agriculture, as detailed in the following paragraphs. On-site experts in both Jordan and Morocco added additional irrigation beyond what the controller calculated if they perceived the crops undergoing stress. Any additional water applications were fed back to the model, as described in Section 2.1.3, and used to estimate the soil moisture for the following day. The inputs used for the POWEIr controller calculations are provided in Appendix Table A.2.

For the Morocco potato season, local Z_r and K_c values were used. The Z_r and K_c values were obtained from the Ministry of Agriculture near Agadir, the Souss-Massa Regional Authority for Agricultural Development (Office Regional de Mise en Valeur Agricole du Souss-Massa or ORMVA-SM). The calculated D_r value was updated at times when the on-site researchers detected that the potato crop was undergoing stress. For the Jordan okra and grape season, Z_r, K_c, and K_y values from literature were used [54,68–71]. The Z_r for okra and grape was measured weekly and linearly interpolated for future calculations, as no detailed root depth measurements were available. On July 21, 2023, the POWEIr controller's D_r and K_c values were updated when it was noted that the okra crop coefficient had been 30% too high due to a clerical error. For the Morocco carrot season, local Z_r and K_c values were obtained from ORMVA-SM. The controller-calculated D_r (Eq. (7)) was not re-calibrated during this season, which more closely represents the desired minimal calibration for the POWEIr controller design. For all crops, the f_w was calculated based on field measurements of the hydraulic system layout and crop properties.

For Level P, the pump pressure setpoint for the section permutations was calibrated by increasing the pump power until the last emitter was operating at its rated flow [64]. The proportional and integral controller gains were tuned for the hydraulic network using standard system identification and PID tuning techniques, which are available as software packages [72–74]. The calibration was conducted by on-site researchers.

3.1.3. Soil moisture measurements

Both experimental setups used wired pressure sensors (ProSense SPT25-20-0060A), a flow meter (ProSense FMM200-1002), a weather station (Ambient Weather WS-2902C), and capacitance-based soil sensors that estimate θ_v directly (Sentek Drill & Drop Probe). Each soil moisture sensor was placed based on best judgment from on-site agronomists to represent typical sensor placement practices in commercial fields. It should be noted that for precise soil moisture measurements it is recommended that up to 25 sensors per half hectare should be used [75]. However, only up to two sensors were used per half hectare to reflect a realistic level of investment that cost-constrained farmers in LMICs could make in precision irrigation, if soil moisture sensors are used at

all. This experimental design therefore enabled a comparison between the controller-derived soil moisture estimates and soil moisture information obtained from a limited number of point sensors.

The soil moisture sensors took measurements at multiple depths. In Jordan, soil moisture sensors were placed in the middle of sections two and six of the controller field near an emitter and the okra crop. Section two had loam soil of a consistent texture and low salt content while section six had sandy clay soil with an inconsistent texture and higher salt content. Due to operational constraints during installation, the sensors in sections two and six were not installed to uniform depths, resulting in measuring profiles of 0 to 41 cm and 0 to 33 cm, respectively. In Morocco, the soil sensors took measurements at 10 cm increments from 0 to 60 cm. During the potato season, only one sensor was used due to malfunctions in the second sensor. This was found to be sufficient for a preliminary comparison to the virtual soil moisture. The single sensor was placed in the middle of the last section of the controller field, section six. During the carrot season, two soil moisture sensors were used in sections one and six.

Bulk soil measurements were taken on the controller fields. The bulk soil measurement conducted in Jordan used the gravimetric method where the soil water content, θ_g, was calculated as

$$\theta_g = \frac{m_{water}}{m_{soil}}, \tag{16}$$

where m_{water} is the mass of the water in the soil in kg, and m_{soil} is the dry mass of the soil in kg. The water mass in the soil was calculated as the difference between the wet soil weight, sampled at multiple locations, and the sample weight after it was oven-dried (m_{soil}). The soil samples in Jordan were collected at a depth of 10 cm over the entire season, and additional 30 cm depth samples were collected towards the end of the season.

The bulk soil measurement taken in Morocco was from ten lysimeters spread evenly across the controller field. The soil water content from the lysimeter was calculated using Eq. (16). The weight of the lysimeter buckets with wet soil and the weight of the buckets with dry soil before the start of the irrigation season (m_{soil}) were compared to obtain m_{water}. For the potato crop, the lysimeters were 60 cm deep, and for the carrot crop the lysimeters were 20 cm deep.

Both the soil sample and lysimeter methods are common agronomic research methods for measuring bulk θ_g. The bulk soil measurements were used as a baseline for evaluating both the soil sensor measurements and POWEIr controller estimations of θ_v. To compare bulk measurements, θ_g was converted to:

$$\theta_v = \theta_g \frac{\rho_{soil}}{\rho_{water}}. \tag{17}$$

Here, ρ_{soil} is the dry bulk density of the soil in kg/m^3 and ρ_{water} is the density of water in kg/m^3. The average θ_v in the root zone was calculated by the POWEIr controller using Eq. (11) and the soil moisture model described in Section 2.1.3. In Morocco, the bulk soil lysimeter measurements from multiple depths were used to calculate an average θ_v. During the potato season, measurements were taken from 0–60 cm, and during the carrot season, measurements were taken from 0–20 cm. The shallower depth made the lysimeter buckets smaller, which facilitated more frequent data collection.

3.1.4. SPDI hardware and operation measurements

In Jordan, both the controller and reference fields used a 2.2 kW pump (Pedrollo pump F32/160B, three phase IE3 motor) and a locally sourced disk filter, sand filter, and fertilizer injector. The controller field was powered by six 540 Wp solar panels (Tiger Pro-JKM540M-72HL4-V). The controller side also had a 10.2 kWh lithium iron phosphate (LFP) battery (DGRID DG-B-WM-48200). The reference field pump was powered by the grid, measured using a grid meter (Carlo Gavazzi EM24); the reference side's data acquisition (DAQ) unit was powered by two 300 Wp solar panels (Jain Irrigation JJ-M672) and two 1200 Wh GEL batteries (NPP NPG12-100Ah–12V, 100Ah).

In Morocco, both the controller and reference fields used a 2.2 kW pump (Sealand CN 32-160B) and had a disk filter. The controller field and reference field were powered by eight 330 Wp panels (Eagle JKM330PP-72-V) each. The controller field had a 7.2 kWh battery capacity using two LFP batteries (Maribat MLFP 48V 3600Wh) to power the irrigation system at times of low solar irradiance, and the DAQ unit at the reference field had two 1200 Wh GEL batteries (EcoGreen 6-GFJ-100–12V, 100Ah) to transmit data at times of low solar irradiance. In both countries, the hydraulic networks were designed and installed in partnership with local irrigation engineers.

The POWEIr controller hardware in each country consisted of a power system hardware manager (Victron Cerbo GX), a maximum power point tracker (Victron Smart Solar MPPT 250V 60A), an inverter (Victron Multiplus 48/5000/70), a battery management system (Victron Smart Shunt 500A/50mV), a DC-DC converter (Victron Energy Orion-Tr 48/24-12), a variable frequency drive, or VFD (DURApulse G S11N-23P0), a programmable logic controller (CLICK PLUS PLC), and an LTE router, modem, and antenna (MikroTik RBSXTR&R11e-LTE and RBD52G-5HacD2HnD-TC). The DAQ unit hardware in each country consisted of a power system hardware manager (Victron Cerbo GX), a maximum power point tracker (Victron Smart Solar MPPT 150V 35A), a battery monitor (Victron Smart Shunt 500A/50mV), a programmable logic controller (CLICK PLUS PLC), and an LTE router, modem, and antenna (MikroTik RBSXTR&R11e-LTE and RBD52G-5HacD2HnD-TC). The DAQ unit in Morocco also included a VFD (Delta VFD MS300 2.2kW) to operate the solar pump on the reference field.

3.2. Simulation methods for irrigation reliability

The aim of the crop yield loss simulation was to characterize the controller's irrigation reliability with a direct drive solar power system. For a direct drive solar power system, which has no battery buffer, irrigation reliability depends on how effectively the controller uses the available solar power to irrigate. Level S is designed to schedule irrigation events such that the pump power closely matches the solar power profile, thereby implementing SPM and minimizing battery use (Eq. (1)). The controller's solar energy use efficiency depends on both the optimization formulation (objective function and constraints) and the solar power prediction accuracy. A metric termed "percent solar fill" (PSF) was created to quantify the controller's solar energy use efficiency when scheduling irrigation events. The PSF for a single day can be expressed as

$$PSF = \frac{E_{pump,DD}}{E_{sol,avail}} \times 100, \tag{18}$$

where $E_{pump,DD}$ is the pump energy Level S schedules under the solar curve, and $E_{sol,avail}$ is the measured solar energy available for pumping.

The yield loss simulation was focused on the performance of the controller software rather than the execution of the irrigation schedule by the user or automation hardware. PSF was defined as the *scheduled* pump energy over the *measured* solar energy to capture both the controller's placement of irrigation events under the solar curve and its solar power prediction error. The *measured* pump energy was not used to calculate PSF as doing so would have incorporated the user- and hardware-related errors that affect the execution of the irrigation schedule.

A sensitivity analysis was conducted to determine how the controller's PSF affected crop yield loss while operating with a direct drive solar power system. First, the PSF was calculated for the experiment systems, removing any irrigation events powered by the battery. The experiment PSF values represent the controller's ability to implement SPM with an appropriately-sized solar array. For the yield loss sensitivity analysis, the average daily PSF over the season was increased to simulate improvements to the controller's solar energy use efficiency. The irrigation amount for the given PSF value was calculated, and the crop yield loss was estimated using the soil moisture model (Section 2.1.3) and experiment input parameters (Appendix Table A.2). For each case,

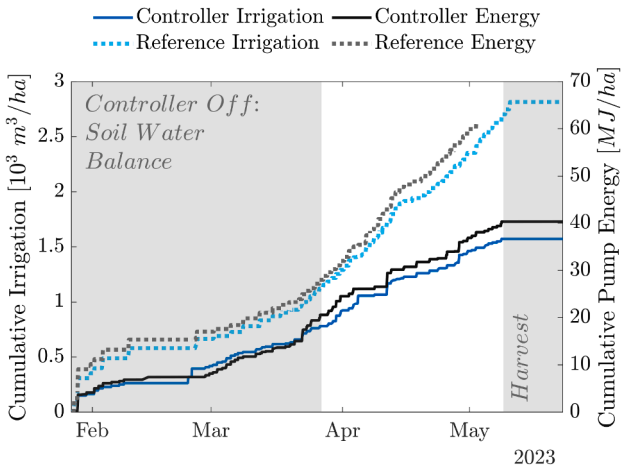

Fig. 3. Cumulative irrigation volume and pump energy comparison between the POWEIr controller and reference fields for the Morocco potato season. The POWEIr controller optimal irrigation scheduling did not start until March 28, 2023. Prior to this (grey box), the controller field was irrigated based on the soil water balance, similar to the theory is Section 2.1.3. The POWEIr controller also did not run during the potato harvest (grey box).

the controller's average daily PSF was increased from the observed experiment value to 100%, or perfect use of the solar energy available for irrigation. This analysis was conducted for the Jordan grape and okra and Morocco carrot seasons. (As previously noted, the irrigation demand of the Morocco potato season was not large enough to necessitate SPM.) The simulated yield loss as a function of PSF was used to assess the controller's irrigation reliability and its impact on solar power system cost.

4. POWEIr controller performance results

4.1. Water, energy use and crop yield

The POWEIr controller exhibited savings of 29%–44% in water use and up to 43% in pump energy consumption compared to local farmers' irrigation practices on the reference fields. Notably, consistent savings were observed across multiple contexts, crop types, soil textures, and levels of automation. The incorporation of an irrigation amount feedback loop enabled the controller to achieve water savings, even when additional irrigation was applied due to user error, extreme temperatures, or to address observed crop stress.

Water savings were achieved even with manual irrigation in Jordan where the irrigation schedule was not perfectly executed. In fact, Van de Zande et al. [48] showed that the schedule was followed correctly for 51% of the scheduled events in Jordan, mostly due to users not being on-site on weekends and holidays. This means that the users in Jordan did not open and close the valves according to the POWEIr controller's schedule about half of the time. Yet, the users reported when they opened and closed the valves (or chose not to) with 93% accuracy. This indicates that there was a large amount of user scheduling error in Jordan, but also users reliably reported the irrigation delivered that was fed back into the POWEIr controller (Fig. 1). This accurate data feedback allowed the controller to update its calculations and deliver sufficient irrigation to the crops over the season. Even with the large user scheduling error the POWEIr controller was able to save water and energy compared to typical practice without compromising crop yield.

4.1.1. Morocco potato season

Fig. 3 shows the cumulative irrigation volume and pump energy used by both the controller field and the reference field during the Morocco potato season from January to June 2023. The reference field's pump power measurement stopped recording on May 3, 2023, so results for the pump energy were compared on this date. The results show the POWEIr controller used 44% less water and saved 38% in total pumping energy compared to the reference field irrigating according to typical practices. The controller and reference potato yields were 23.7 tonne/ha and 26.2 tonne/ha, respectively. The controller field's 10% reduction in yield compared to the reference field could be attributed to the respective quality of the water used on each field. Electrical conductivity (EC) of the water on the controller field was measured to be 2.4 dS/m during this season, which represents a salinity level sufficient to cause up to a 25% reduction in potato yield (2.5 dS/m) relative to a non-stressed crop [76]. The EC of the water on the reference field, measured to be 1.4 dS/m, was between the thresholds reported to cause no reduction (1.1 dS/m) and up to a 10% reduction (1.7 dS/m) in potato yield [76]. Therefore, the lower yield on the controller field could be accounted for by the higher salinity of the water. The WUE was 15.1 kg/m^3 for the controller field and 9.3 kg/m^3 for the reference field, a 62% improvement in WUE by the controller. This means the controller saved a considerable amount of pumping energy and water compared to typical drip irrigation practices while maintaining a similar crop yield, given the difference in water salinity.

4.1.2. Jordan okra and grape season

Fig. 4a shows the cumulative irrigation volume and pump energy used by both the controller field and the reference field, which was irrigated based on a well-practiced farmer's recommendations, during the Jordan okra and grape season from May to December 2023. From May 28, to July 21, 2023, the crop coefficient selected for the okra was inadvertently 30% higher than required (Section 3.1.2); during this time, the irrigation amounts and pumping energy between the fields were similar. The rainy season started on November 15, 2023, after which little irrigation was required. Additionally, November 15, to December 15, 2023 was a window of time when okra farmers in the region typically finish harvesting okra. Thus, the end of the okra season could have happened at any point during this window. The comparison of performance metrics between fields varies depending on the assumed end of the okra season. Therefore, instead of assuming a single end-of-season date, results are presented for the earlier and later end-of-season dates. The results show that if the end of the okra season is assumed to be November 15, 2023, the controller used 42% less energy and 40% less water than the reference field. If the end of the season is assumed to be December 15, 2023, the controller's energy savings increased to 43% and water savings remained the same.

The grapes were young grape vines and did not produce any yield on either field. Fig. 4b shows that the okra started producing yield on July 18, 2023 until the end of the season. The the controller field and the reference field had okra yields on November 15, 2023 of 11.0 tonne/ha and 10.8 tonne/ha, respectively. At this assumed end of the season, the okra yield for the controller field was 2% greater than the reference field's yield. The difference in the cumulative okra yield between the controller and reference fields varied between -21%–11% over the season. Assuming the end of the okra season was December 15, 2023, the yields for the controller and reference fields were 11.0 tonne/ha and 11.8 tonne/ha, respectively, or 7% less for the controller field. The controller field stopped producing okra by November 17, 2023 whereas the reference field produced an extra tonne of okra through December 15, 2023. The extension of the okra season for the reference field could be because more irrigation was applied during the season. Even though the reference field had a slightly higher okra yield, its WUE ranged from 0.65 to 0.71 kg/m^3 over the end of the okra season, whereas the WUE stayed at 1.11 kg/m^3 for the controller field. The 56%–71% higher WUE means the POWEIr controller saved significantly in pumping energy and water compared to typical drip irrigation practice for comparable okra yields.

(a) Cumulative irrigation volume and pump energy for okra and grape

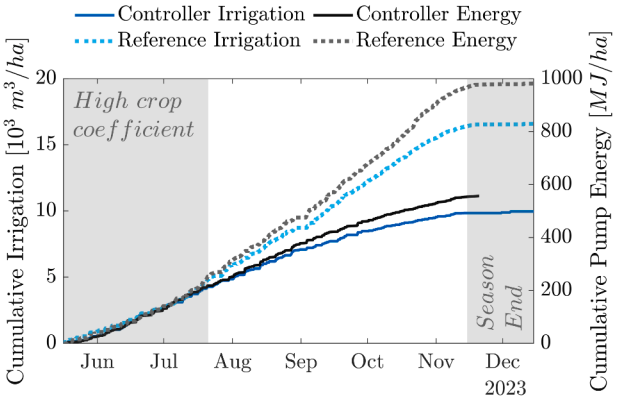

(b) Cumulative yield for okra

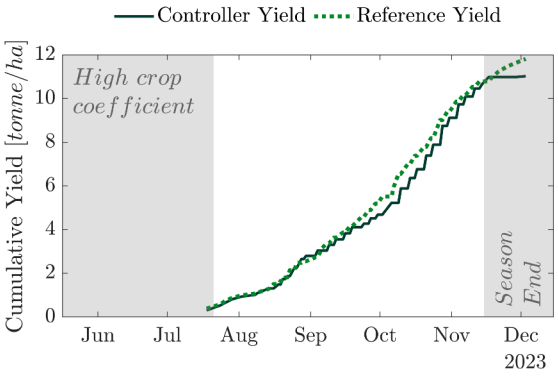

Fig. 4. Cumulative irrigation volume, pump energy, and okra yield comparison between the POWEIr controller and reference fields for the Jordan season. The crop coefficients for the okra crop were set 30% too high and later adjusted on July 21st, 2023 (grey box). Harvesting of the okra began on July 18th, 2023, and continued until the end of the season. The end of the okra season (grey box) could have happened anytime from November 15, to December 15, 2023.

4.1.3. Morocco carrot season

Fig. 5 shows the cumulative irrigation volume and pump energy used by both the controller and reference fields during the Morocco carrot season from July to November 2023. The step changes in the POWEIr controller cumulative irrigation in mid-August and mid-October (Fig. 5, solid blue line) are due to additional irrigation applications recommended by the on-site research partners. The crops were temperature stressed due to extreme temperatures (over 50 °C) starting on August 11th; because of this, additional irrigation was applied on August 12th, August 14th, and August 19th, 2023. Also, on-site researchers applied additional irrigation on October 9th and October 18th, 2023.

At the start of the carrot harvest, on October 26, 2023, the controller had used 25% less water than the reference field, but used 10% more energy. The POWEIr controller stopped calculating the daily irrigation schedules on October 26th, 2023, after which on-site researchers irrigated the carrots to facilitate harvesting and keep the carrots fresh to sell in the markets. The water savings increased to 29% by the end of the carrot harvest, but the controller stopped recording pump data on October 26th, 2023, so no additional energy consumption was recorded.

The increase in energy use on the controller field can be attributed to hardware selection. When implementing SPM, the pump operates over a range of flow rates, and due to the hydraulic pipe network physics, an increase in flow rate corresponds to a non-linear increase in pumping power [67]. In addition, a pump's efficiency can vary significantly across its operating range depending on the selected pump model and system operating points. For the experiments, the controller could operate up to two field sections at once, and the pump operated at about 61% efficiency for one section and 45% efficiency for two sections; the lower efficiency corresponds to the higher pump operating power. On the reference field, which only operated one section at a time, the pump efficiency was 57% with a standard deviation of 5% (SD = 5%). Cumulative pump energy consumption and efficiency measurements for both fields are provided in Appendix Figs. A.1 and A.2, respectively. The variation in pump operating power and efficiency with SPM could account for the increase in energy consumption on the controller field compared to the reference field.

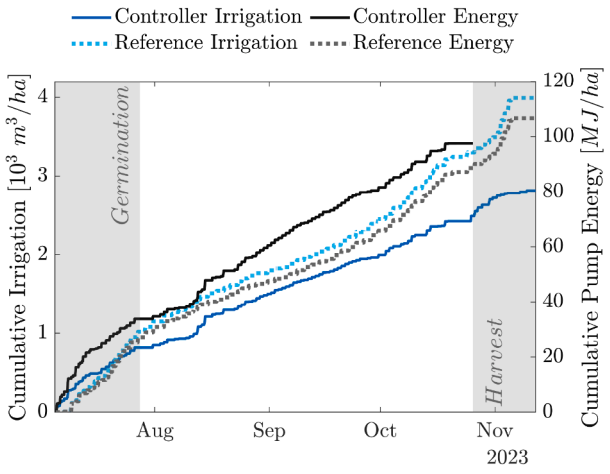

Fig. 5. Cumulative irrigation volume and pump energy comparison between the POWEIr controller field and reference fields for the Morocco carrot season. Morocco experienced an extreme heat wave during this season and additional irrigation was added to the controller field by on-site researchers on August 12th, August 14th, and August 19th, 2023. The controller did not determine irrigation amounts during carrot germination or harvest (grey boxes).

This result highlights an important trade-off to consider when implementing SPM schedules. The POWEIr controller is designed to target power system cost in two ways: 1. reduce the total irrigation water volume, thereby targeting a lower total pumping energy over the season, and 2. implement mutli-section operation to use solar energy as efficiently as possible (i.e., SPM) and minimize the required power system capacity. While in the previous use cases these two aims did not conflict, under certain operating conditions, the SPM schedule may increase pump energy consumption compared to an SSO reference due to the variable pump efficiency and operating powers with multi-section operation. A solar power system with the controller's SPM schedule could still eliminate the need for grid power or fuel, which would ultimately reduce farmers' operating costs. However, this result elucidates how hydraulic system design, pump selection, and the maximum number of sections allowed for SPM could impact the SPDI system performance.

At the end of the carrot season, a soil sample was taken that indicated a severe parasitic nematode infestation of 253 Meloidogyne species per 100 g of soil at the controller field. Likely due to the infestation, the controller yield was 44% lower than the reference yield. It has been shown that root-knot nematode infestations can cause between 25%–45% reduction in carrot yield, with a potential for total yield loss [77–81]. Additional yield reduction could have been caused by a difference in water quality between the controller field and reference field. EC of the water at the controller field could have contributed to a 15% greater reduction in carrot yield compared to the EC of the water at the reference field [76]. Although a large loss in yield occurred on the controller field, a sample of the best carrots from each field showed that similar yields were possible. A sample of 50 carrots per section was taken from

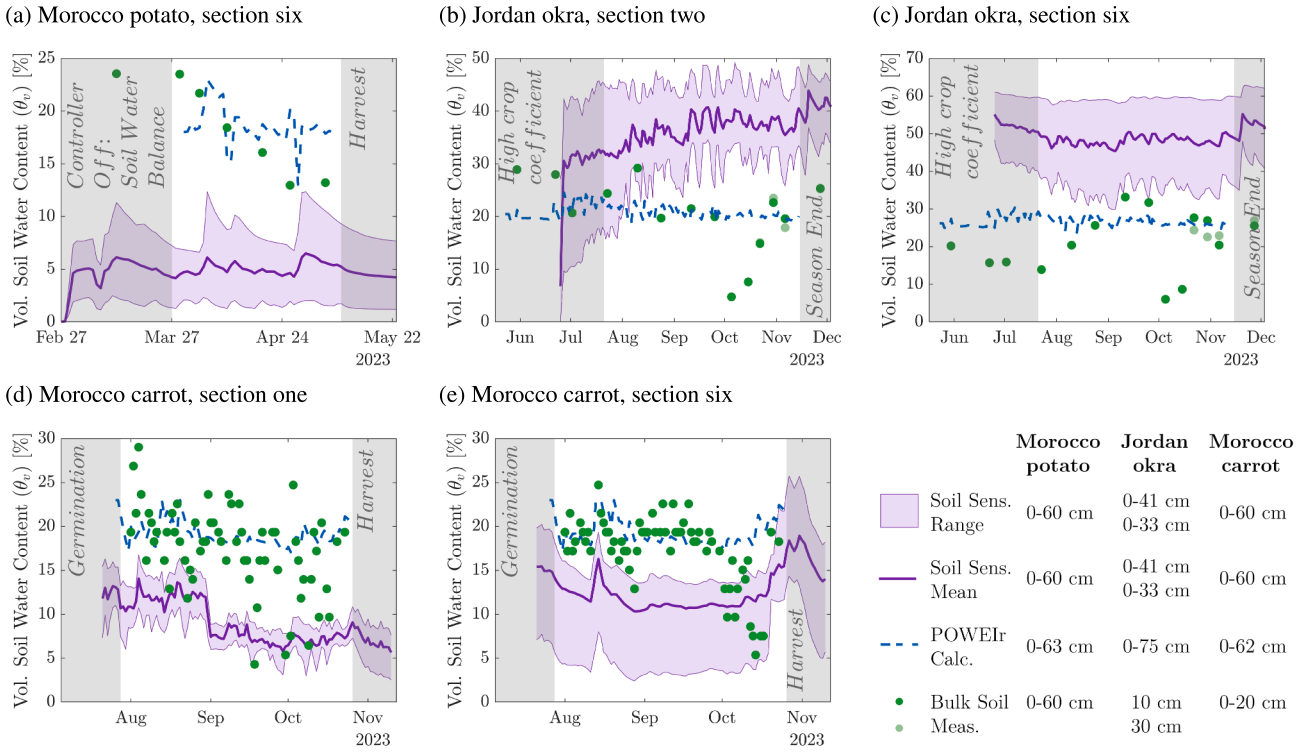

Fig. 6. Volumetric soil water content (θ_v) comparison. Estimates from the POWEIr controller (blue dashed line) compared to the full range and average soil sensor readings (purple area and line) and in-field bulk measurements (green dot) for the farms in Morocco and Jordan. The legend summarizes the depth(s) at which each measurement was taken. In Morocco, **a** and **e** show the θ_v for section six, and **d** shows the θ_v for section one of the controller field (corresponding to Fig. 2); lysimeters were used to take the bulk θ_v measurements. In **a**, **d**, and **e** the grey boxes show times that the controller wasn't running during crop germination, harvest, or when the controller wasn't fully set up and researchers implemented a soil water balance to irrigate. For the potato season (**a**) only the section six soil moisture sensor was operational. Both sections' sensors were working for the carrot season (**d** and **e**). In Jordan, **b** shows the θ_v for section two with the soil sensor measuring at depths of 0–41 cm. **c** shows the θ_v for section six with the soil sensor measuring at depths of 0–33 cm. In Jordan, the bulk θ_v was measured using the gravimetric method with oven drying from soil samples taken at 10 cm. Four bulk soil samples were also taken at 30 cm (light green dots) at the end of the season in both sections. In **b** and **c** the grey boxes show when the crop coefficient and the controller's irrigation amounts were artificially high due to a clerical error and the end of the season when the controller was off. (For interpretation of the references to colour in this figure legend, the reader is referred to the web version of this article.)

each field and the best samples from the controller field and reference field both had weights of 0.2 kg. The similarities in the best carrot sample weight indicate that, without the pest and water quality issues, the total yield of the controller and the reference fields could have been comparable. The measured WUE was 4.89 and 6.12 kg/m^3 for the controller and reference fields, respectively. However, with similar yields, the controller field's WUE would have been 8.68 kg/m^3, or 42% higher than the reference field.

4.2. Soil moisture accuracy

Fig. 6 shows the θ_v that the POWEIr controller estimated compared to the soil sensors and bulk soil measurements for the various Morocco and Jordan crop seasons at the sections where the soil sensors were located.

Fig. 6a shows the θ_v results for the Morocco potato season. The POWEIr controller bulk θ_v calculations were on average 2% (SD = 5%) higher than the lysimeter bulk measurements. The POWEIr controller calculated D_r was reset based on the lysimeter measurements when on-site researchers detected crop stress. The D_r values were reset on March 30, April 10, and April 27, 2023. This could have helped the POWEIr controller estimations of θ_v more closely match the bulk soil measurements. The soil moisture sensor reported 13% (SD = 5%) lower θ_v averaged over all depths compared to the bulk soil measurements. The inaccuracy in the soil sensor was most likely due to a placement issue: either it was not placed close enough to where the water from the emitter was, or it was placed in a patch of soil that was dry due to emitter malfunction or variability in the soil. Soil moisture sensors are prone to placement issues and, to get an understanding of what is happening in the bulk of the soil, multiple sensors are necessary [75,82].

Fig. 6b and c show the θ_v results for the Jordan okra and grape season. Despite a difference in soil texture, the POWEIr controller calculations are shown to match well with the bulk measurements. The controller θ_v calculations were on average 1% (SD = 7%) and 6% (SD = 8%) higher than the bulk soil measurements for sections two and six, respectively. It should be noted that the bulk measurements were taken at 10 cm depth whereas the controller calculated the θ_v up to the root zone depth, which went up to 75 cm for the okra. The large difference in depths implies using the bulk soil measurements may not be a direct comparison. However, four out of fourteen of the bulk soil measurements were taken at 30 cm and shown to be 0.2% (SD = 1%) and 1% (SD = 3%) lower compared to the 10 cm measurements for sections two and six, respectively. The small difference in θ_v between depths demonstrates that the 10 cm measurements may have been a good indicator of the θ_v at higher depths. The soil moisture sensors reported 17% (SD = 8%) and 27% (SD = 9%) higher θ_v averaged over all depths compared to the bulk θ_v measurements for sections two and six, respectively. The larger difference in the θ_v of the soil sensor suggests that it under-performed compared to the POWEIr controller estimates.

Fig. 6d and e show the θ_v results for the Morocco carrot season. The POWEIr controller θ_v calculations were on average 2% (SD = 5%) and 2% (SD = 4%) higher than the lysimeter bulk measurements for sections one and six, respectively. This small difference indicates good agreement between the POWEIr controller calculations and lysimeter

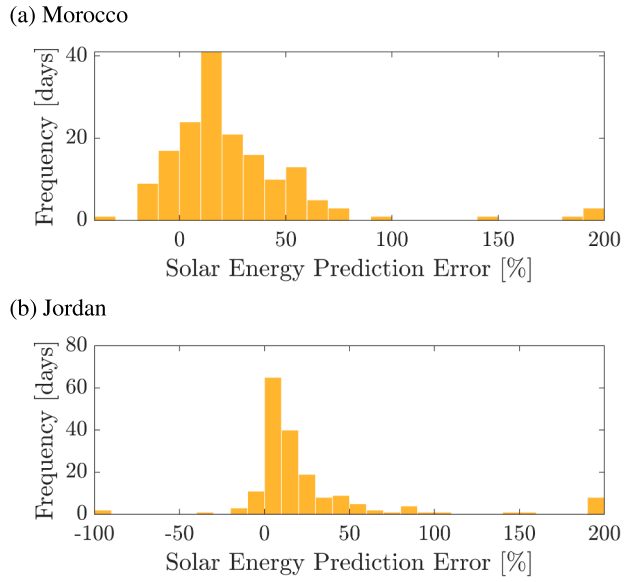

Fig. 7. Daily solar energy prediction error for Morocco and Jordan. The error is the difference between the energy under the predicted solar power curve and the energy under the solar power curve calculated from the measured weather data. The energy error was calculated daily and made into a histogram for **a**, both potato and carrot seasons in Morocco, and for **b**, the okra and grape season in Jordan.

measurements, although it should be noted that they were taken at different depths. The θ_v for depths up to 20 cm may differ compared to depths up to 62 cm due to climate conditions and soil stratification. Yet, the soil moisture sensor reported 8% (SD = 4%) and 6% (SD = 4%) lower θ_v averaged over all depths compared to the bulk soil measurements for sections one and six, respectively. The closely matching data for the θ_v between the 60 cm soil sensors and the 20 cm lysimeters indicate that the shallower measurements may have been close to the θ_v at higher depths. Therefore, the POWEIr controller calculations may have been accurate even to higher depths.

4.3. Controller prediction error

The solar prediction error was calculated by comparing the Level S daily predicted solar energy to the measured solar energy. The daily percent error between the predicted solar energy and the calculated solar energy from the weather data is shown in Fig. 7.

The solar prediction error was calculated for the duration of the experiment. For Morocco (Fig. 7a) the mean solar energy prediction error was 32% (SD = 93%). For Jordan (Fig. 7b) the mean solar energy prediction error was 31% (SD = 68%). Although the mean solar prediction error was around 30% for both countries, there was a large SD, meaning there were many days when the solar prediction error was much higher. The histograms are shown to be skewed positive, signifying the POWEIr controller often over-predicted the daily available solar energy. As the controller's predictions were based on a linear interpolation of hourly data, the model did not capture fluctuations, such as those due to clouds, which added to the error.

In addition to solar power prediction error, other sources of error were user choice or mistakes operating manual valves (Section 4.1) and hardware failures. In Jordan, where an engineer operated the irrigation section valves manually following instructions in the app, there were mistakes and delays in valve opening as well as choices made by the engineer due to other agronomic factors [48]. Furthermore, during particularly hot days, there were instances where the pump VFD overheated, leading to a sharp decline in electronic efficiency, which increased the pump power above the calibrated operating points. Both user and hardware related errors contributed to scheduling errors in terms of pump power. The most unfavorable uncertainty condition was when Level S over-predicted the available solar power and under-predicted the required pump power; without a buffer battery, this scenario would result in a failed irrigation event because there would be insufficient solar power to operate the pump. The following section explores the impact of this scheduling uncertainty on irrigation reliability.

4.4. SPDI reliability and cost with the POWEIr controller

The PSF, which describes the controller's solar energy use efficiency, was recorded for both countries. For the Jordan okra and grape season, the controller's average daily PSF was 30% (SD = 20%), and for the Morocco carrot season, the controller's average daily PSF was 39% (SD = 20%). This means that, on average, the controller's optimized schedule only used about a third of the daily available solar energy. The large standard deviation in both cases suggests that the irrigation schedule varied significantly day to day. Despite the controller producing SPM schedules, these observed PSF values suggest a low solar energy use efficiency.

To demonstrate the source of these low PSF values, Fig. 8 shows the optimized irrigation schedule, predicted solar power, and measured solar power for two sample days in each country. In Jordan, the PSF was 27% on July 12th and 52% on July 13th. In Morocco, the PSF was 72% on September 2nd and 36% on September 3rd. These sample days show that both the placement of the irrigation events by the Level S optimization and the solar power prediction error contributed to the controller's low average PSF. In Jordan, although there was sufficient solar power to execute the irrigation schedule on both days, Level S placed irrigation events at the beginning and end of the day, where the controller over-predicted the available solar power. In the middle of the day, when solar power was abundant, Level S allowed for gaps between irrigation events. On September 2nd in Morocco, the controller effectively implemented SPM, leading to a higher PSF, but the solar power variability reduced the power prediction accuracy. On the following day, the Level S optimization spread out the irrigation events, leading to a lower PSF. Without a battery, the controller would be less able to accommodate such power prediction errors and irrigate reliably.

To quantify the controller's irrigation reliability without a battery, the crop yield loss was simulated for a direct drive solar power system using the experiment PSF values. The estimated yield loss was 10% for grapes, 46% for okra, and 17% for carrots, which suggests the controller would have underperformed compared to the reference fields without the battery as a buffer power source. Although the first term of the Level S objective function penalizes battery use (Eq. (1)), the yield loss simulation suggests that this term was insufficient to encourage SPM. Modifying the Level S optimization to more effectively cluster irrigation events under the solar curve could increase the controller's average PSF and enable reliable irrigation with direct drive solar. Adding a constraint or objective function term that specifically penalizes gaps between scheduled irrigation events could increase the controller's PSF. Alternatively, for systems with automatic valves, Level S could optimize the irrigation schedule over a shorter time horizon to enable real-time SPM adjustments.

Crop yield loss was simulated for a range of PSF values to estimate how much the average PSF would need to be increased to eliminate the battery. The controller's average PSF was increased from the experiment values (30% for Jordan, 39% for Morocco) to 100%, or perfectly matching the pump operation to the solar power profile. Fig. 9 shows the normalized crop yield as a function of the increase in average PSF. On the x-axis, zero represents removing the battery at the experimental PSF values, which resulted in the estimated yield loss reported above. Moving right along the x-axis represents increasing the use of the available solar energy for scheduled irrigation events, or increasing the controller's average PSF. For the sample days shown in Fig. 8, this could mean placing the early- and late- scheduled irrigation events in the middle of the day

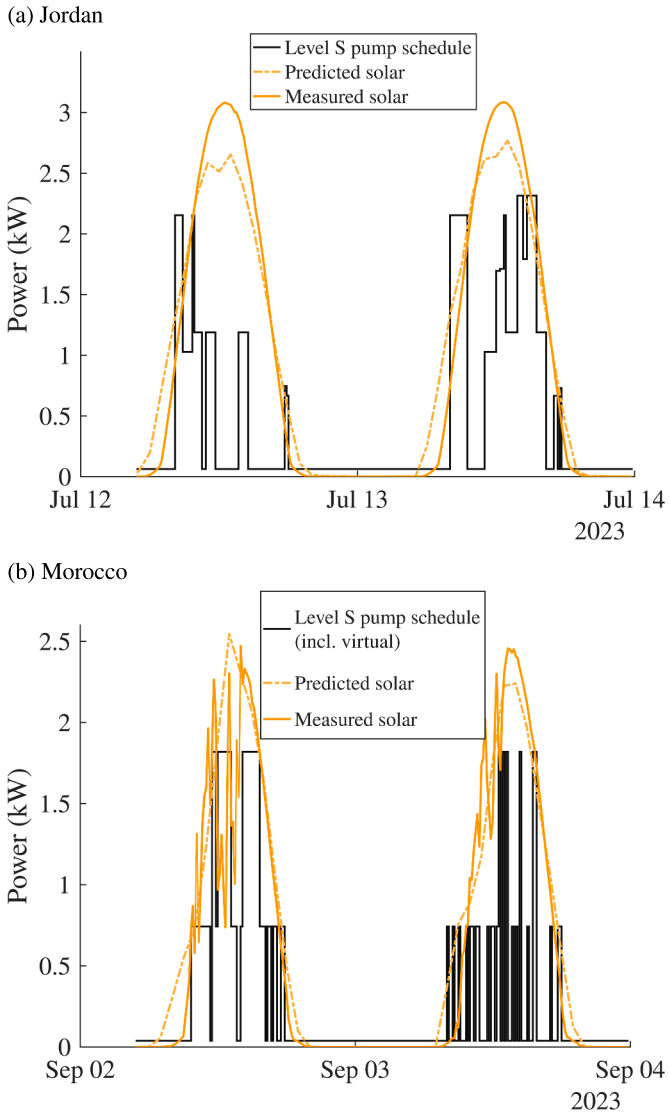

Fig. 8. Level S optimized schedule, solar power prediction, and measured solar power on two sample days for **a** Jordan grape and okra and **b** Morocco carrot (real and virtual field sections). In Jordan, the controller's percent solar fill (PSF) was 27% and 52% on July 12th and 13th, respectively. In Morocco, the PSF was 72% and 36% on September 2nd and 3rd, respectively. Irrigation events that fall outside the solar curve are not included in the PSF metric as these events would require a battery buffer. The Level S optimization allowed for gaps in the irrigation schedule, which led to low solar energy use efficiency on average.

to avoid using the battery. As the solar energy use increases, the irrigation volume delivered with direct drive solar increases, and the crop yield approaches its maximum.

Fig. 9 shows that increasing the controller's average PSF could enable reliable irrigation (>0.99 normalized yield) without a battery. The diminishing return in crop yield as PSF is increased suggests that there is room for some uncertainty in the controller's irrigation scheduling with direct drive solar. In Jordan, an average PSF of 72% would produce maximum yield for the intercropped grapes and okra. In Morocco, an average PSF of 79% would produce maximum yield for the carrots. For both cases, this means increasing the controller's average solar energy use by about 40% ($\Delta PSF = 42\%$ for Jordan, $\Delta PSF = 40\%$ for Morocco). Without this change, the solar panels and battery capacity required to irrigate reliably would cost 2474 USD for Jordan and 2401 USD for Morocco. The battery capacity was calculated based on the remaining daily pumping energy that could not be fulfilled by direct drive solar. Eliminating the battery by increasing PSF would reduce the power system cost by 33% and 46% for Jordan and Morocco, respectively. Conversely, to irrigate reliably with direct drive solar at the experiment PSF values, the solar capacity would need to be increased by over four-fold in both cases. This is because the solar array would have to be over-sized to accommodate the gaps in the irrigation schedule (Fig. 8a). In terms of SPDI system design, adjusting the controller software to increase PSF is more cost-effective than using a solar-battery power system or over-sizing the solar array to accommodate Level S prediction errors and schedule placement issues.

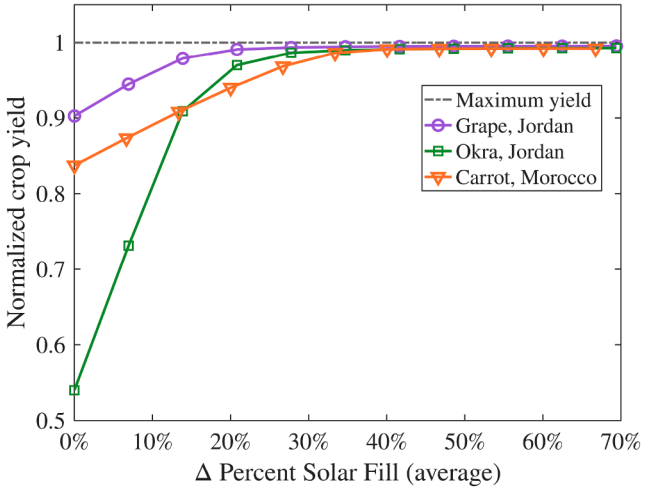

Fig. 9. Simulated crop yield as the controller's percent solar fill (PSF) was increased from the experiment average PSF (30% for Jordan, 39% for Morocco) to perfect SPM with a direct drive solar power system. Increasing the PSF represents the controller scheduling more irrigation events under the solar curve, which leads to greater crop yield. Increasing the average daily PSF by about 40 percentage points in both cases mitigated crop yield loss with direct drive solar.

The yield loss sensitivity analysis also demonstrates that the PSF required for reliable irrigation is a function of crop water sensitivity and field size. Based on their yield response factors (K_y) the crops in order of increasing water sensitivity are grape, carrot, and okra (Appendix Table A.2). This effect can be seen in the slope of the normalized yield curves for grape and okra in Fig. 9. Okra were more responsive to the increased irrigation amount than grapes. This suggests that PSF may be an important controller performance metric for highly water sensitive crops. A compounding factor is field size, and therefore, daily irrigation time. Larger farms require longer total irrigation times to meet crop water demand. For a system with longer irrigation times, there would be fewer time-slots in a given day to increase PSF by rearranging the irrigation events. The Morocco controller field had a larger area (including the virtual sections) and a longer daily irrigation time (6 h/day) than the Jordan field. This is why a greater increase in PSF was required to mitigate the carrot yield loss in Morocco compared to the grapes and okra in Jordan despite carrots having the intermediate water sensitivity (Fig. 9). This suggests that field size as well as crop water sensitivity could determine the PSF required to irrigate reliably with a direct drive solar power system. Therefore, defining a PSF target specification that is a function of both crop type and field size could facilitate improvements to the controller software design.

5. Discussion

The performance validation of the POWEIr controller demonstrates its potential as an accessible precision irrigation tool for farmers in LMICs. The results show that the proposed controller, with its physics-based models, minimal sensor reliance, and machine learning algorithms, has the potential to improve resource use efficiency, accurately

calculate crop water demand with minimal intervention, and enable low-cost solar power systems. These findings are aligned with UN SDG 2, achieving food security and promoting sustainable agriculture, and SDG 13, taking action to combat climate change. If adopted widely, the POWEIr controller could contribute towards SDGs 6 and 7, which focus on sustainable water management and access to affordable sustainable energy.

The controller's performance was validated against target specifications identified by Van de Zande et al. [16]. To be valuable and accessible to resource-constrained farmers, the controller had to:

- Reduce water use by 10%–50%, comparable to existing irrigation control solutions;
- Increase energy use efficiency by 10% compared to current irrigation practices;
- Accurately compute irrigation volume required to meet crop water demand;
- Ensure reliable operation with a solar power system.

Due to the risk-averse nature of the target users, the controller had to meet these targets while keeping the user in the control loop. The controller also had to be able to function with manual or automatic valves to accommodate varied user expertise and equipment access.

In the experimental validation, the controller reduced water use by 29%–44% across three different crops and growing seasons compared to typical irrigation practices, which puts its performance in the range of existing precision irrigation controllers [83]. The controller improved system WUE by 42%–71%, demonstrating its ability to reliably meet crop water demand, and field measurements showed that the controller was able to accurately estimate soil moisture content for different crop and soil types with minimal intervention. The controller reduced pump energy consumption by up to 43% compared to typical irrigation practices for two of the experiment cases. This suggests that the controller could enable low-cost solar power systems, which could lower farmers' energy costs in the long term compared to grid or fuel. For the third case, the controller used 10% more energy than the reference field due to SPM and variable pump efficiency with multi-section operation. This increase in pump energy use could be mitigated through pump selection and minimizing efficiency losses in the electronics hardware for future iterations of the controller.

Although the experimental systems relied on a battery buffer for irrigation, the yield loss simulation results suggest that an adjustment to the Level S objective function could enable reliable direct drive solar, reducing the power system cost. The Level S optimization could be updated to penalize time gaps between irrigation events—rather than just penalizing battery use—to maximize solar use for irrigation. Another option would be to add the capability for real-time SPM schedule adjustments. The controller already has the capability to adjust its daily schedule based on feedback about previously delivered irrigation. Shortening the MPC prediction horizon to optimize the irrigation schedule more frequently could increase PSF and mitigate prediction errors. This real-time optimization may only be feasible for farms with automatic valves as the schedule adjustments may be difficult to implement manually. To mitigate controller prediction errors for manual systems, the weather forecast model, electronics hardware efficiency, and app-based user interface could be further refined.

The results showed that, for the experiment use cases, changing the controller software was more cost-effective than using a solar-battery power system or an over-sized direct drive solar power system to accommodate Level S scheduling gaps and prediction errors. Additionally, it was found that the PSF metric, which describes the controller's solar energy use efficiency, could be used to characterize the controller's irrigation reliability as a function of crop water sensitivity and field size. Therefore, the PSF required for reliable irrigation under a certain set of operating conditions could become a design specification for future iterations of the controller.

This study demonstrates the feasibility of an irrigation controller that keeps the user in the control loop while improving resource use efficiency. As such, the findings of this study could expand the potential user base for precision irrigation technologies and encourage designers to explore solutions that meet the needs of resource-constrained farmers. Furthermore, this study may motivate further investigations into sensorless parameter estimation in agriculture to facilitate low-cost, accessible control solutions for a broader market. Refining the POWEIr controller based on the findings of this study could increase the adoption of sustainable irrigation practices.

5.1. Limitations and future work

The controller prototype in this study used hardware and calibration techniques that are potentially inaccessible in LMICs. Higher-cost, research-quality hardware, including the power and battery monitoring units and control, inverter, and MPPT, was used for data collection. Future work will aim to reduce the cost of the POWEIr controller hardware and confirm that similar results can be achieved. Additionally, the power systems used in this study were oversized to support not only the irrigation system but also the data collection. Future work could investigate optimized solar power system sizing and evaluate the relationship between total solar energy generation and pump energy consumption. The crop parameters used in this study were tuned based on the advice of local irrigation engineers and agronomists. Farmers may not have access to expert advice, so future iterations of the POWEIr controller must meet its performance targets without relying on parameter tuning by agronomists. Future work could explore building a database of local crop parameters that are proven to work well with the controller or incorporating crop image-based feedback with the phone application for more accessible parameter tuning.

Future controller design features were noted during the experiment. Irrigation volume and fertilizer requirements are closely tied, but fertilizer calculations have not yet been included in the POWEIr controller. Future work should explore incorporating fertilizer schedules with the POWEIr controller. A robust, repeatable Level P calibration procedure will need to be developed to ensure the pump pressure set points are accurately identified despite topographical variations on the field. A more advanced version of the POWEIr controller could incorporate dynamic time steps for seasonal and temperature variations that allow the controller to adjust to growth, evapotranspiration rates, and soil and salinity changes. Future work should characterize the PSF metric under a variety of operating conditions, particularly related to crop water sensitivity, field area, and daily irrigation time. The controller could also incorporate a more detailed soil mechanics model and treat water stored in the soil as a buffer, in place of a battery, to mitigate scheduling uncertainty with direct drive solar.

Finally, this study tested the POWEIr controller in the MENA region, but it has been shown that such a controller could be beneficial in regions where the use of irrigation in general is relatively low, such as East Africa [16]. Future work should explore the implementation of the POWEIr controller in East Africa and additional markets.

6. Conclusions

To improve global food security, it is imperative to intensify crop production using existing resources. Current sustainable agriculture technologies require technical expertise to operate and are cost-prohibitive to farmers in LMICs. This study proposes the Predictive Optimal Water and Energy Irrigation (POWEIr) controller as a solution that could meet the needs of resource-constrained farmers.

Unlike existing precision irrigation control solutions, the POWEIr controller uses minimal field sensors and relies on case-specific physical models to produce optimized irrigation schedules for solar-powered drip systems. The controller concurrently optimizes system water and

energy use, which to the authors' knowledge, is a novel approach relative to existing precision irrigation controllers. Additionally, the POWEIr controller was shown to increase resource use efficiency while keeping the farmer in the decision-making loop, a necessary feature to build trust with highly risk-averse users. This is a departure from common practice in precision control design, which typically aims for full automation to achieve system performance objectives.

This paper presents the experimental validation of the POWEIr controller on small-scale farms in Jordan and Morocco. The controller was tested under various operating conditions with diverse crop and soil types. The results demonstrate the controller's potential for water and energy conservation with minimal adverse effect on crop yield. In addition, this study characterizes the controller's irrigation reliability and its impact on SPDI power system cost. The POWEIr controller was able to reduce water use by up to 44% and pump energy consumption by up to 43% compared to local farmers' drip irrigation practices with minimal impact on crop yield. The results suggest that the controller could meet the target specifications identified by Van de Zande et al. [16] for a precision irrigation controller in resource-constrained markets. The study also elucidates future adjustments to the POWEIr controller software that could increase its operational reliability and decrease SPDI power system cost.

This work demonstrates the feasibility of a precision irrigation controller designed for LMIC contexts that could be both technologically and economically accessible to farmers. With further refinements, the POWEIr controller has the potential to expand sustainable irrigation practices and increase the adoption of SPDI in these markets.

Funding

This research was funded by the K. Lisa Yang Global Engineering and Research (GEAR) Center at MIT, a gift from the Julia Burke Foundation, and the United States Agency for International Development (Cooperative Agreement Number AID-OAA-A-16-00058).

CRediT authorship contribution statement

Carolyn Sheline: Writing – review & editing, Writing – original draft, Visualization, Validation, Software, Methodology, Investigation, Formal analysis, Data curation, Conceptualization; **Fiona Grant:** Writing – review & editing, Writing – original draft, Visualization, Validation, Software, Methodology, Investigation, Formal analysis, Data curation, Conceptualization; **Georgia van de Zande:** Writing - review & editing, Software, Methodology, Investigation, Data curation, Conceptualization; **Shane Pratt:** Software, Methodology, Data curation; **Samer Talozi:** Writing – review & editing, Validation, Resources, Project administration, Methodology, Investigation, Funding acquisition, Data curation; **Ammar Namarneh:** Resources, Methodology, Investigation, Data curation; **Anas Mansouri:** Resources, Investigation, Data curation; **Ahmed Wifaya:** Resources, Investigation, Data curation; **Vinay Nangia:** Writing – review & editing, Resources, Project administration, Methodology, Investigation, Funding acquisition, Data curation; **Susan Amrose:** Writing – review & editing, Resources, Project administration, Methodology, Funding acquisition, Conceptualization; **Amos G. Winter V:** Writing - review & editing, Resources, Project administration, Methodology, Funding acquisition, Conceptualization.

Data availability

Data will be made available on request.

Declaration of competing interest

The authors declare the following financial interests/personal relationships which may be considered as potential competing interests:

Acknowledgments

The authors would like to thank our field partners—International Center for Agricultural Research in the Dry Areas (ICARDA) and the National Institute of Agricultural Research (INRA) in Morocco, and Methods for Irrigation and Agriculture (MIRRA) in Jordan—for coordinating field activities, facilitating field installations and data collection, and advising on local best practices and agronomy resources.

Appendix A.

A.1. Level S optimization bounds and constraints

The Level S irrigation optimization is subject to the physical bounds and dynamic constraints described in Sheline et al. [18]. The control variables are subject to the following physical bounds at each time step, i or n:

$$0 \le u_{1,i} \le 1, \tag{A.1}$$

$$-1 \le u_{2,i} \le 0, \tag{A.2}$$

$$d_{s,i} \in \{1, 0\}, \tag{A.3}$$

$$0 \le x_{s,n} \le 1, \tag{A.4}$$

$$SOC_{min} \le SOC_i \le SOC_{max}, \tag{A.5}$$

$$x_{s,0} = x_{s,ini}, \tag{A.6}$$

$$SOC_0 = SOC_{ini}, \tag{A.7}$$

where $SOC_{\min}$ is the maximum depth of discharge recommended by the manufacturer and $SOC_{\max}$ is the maximum state of charge, typically 1. The initial state of the soil water depletion, $x_{s,ini}$, and battery state of charge, SOC_{ini}, are measured input parameters: SOC_{ini} is measured from the battery at the start of the day and $x_{s,ini}$ is calculated based on Eq. (7) and the previous day's agronomy parameters, measured weather, and delivered irrigation. The $x_{s,ini}$ for the start of a crop season can be estimated from measured soil moisture.

The optimization is also subject to constraints on the system dynamics. These dynamics include changes in the amount of water stored in the soil and the amount of energy stored in the battery. The model for the water stored in the soil is the daily soil water balance. The soil water balance is calculated by solving for x as the fraction of D_r over TAW:

$$x_{s,n} = \frac{TAW\, x_{s,n-1} - Pr_n + RO_n - \frac{1000 I_{del,s,n}}{A_s f_w} + \frac{ET_{c,s,n}}{1-f_{d,s,n}}}{TAW + \frac{ET_{c,s,n}}{1-f_{d,s,n}}}. \tag{A.8}$$

The irrigation delivered in Eq. (A.8) is calculated as

$$I_{del,s,n} = \sum_{i=\delta t}^{i=N_{hor}} d_{s,i} q_s \delta t. \tag{A.9}$$

The battery storage dynamic model is

$$SOC_i = SOC_{i-1} + \frac{u_{max}}{C_{batt}} (u_{1,i} + u_{2,i}) \delta t. \tag{A.10}$$

The battery charging and discharging rates are modeled as functions of ΔP_i, the difference between available solar power and the pump power demand at time step i:

$$\Delta P_i = P_{avail,i} - P_{pump,i}, \tag{A.11}$$

$$u_{1,i} \le \frac{\eta_{batt}}{2u_{max}} \left(|\Delta P_i| + \Delta P_i \right), \tag{A.12}$$

$$u_{2,i} = \frac{1}{2u_{max}\eta_{batt}} \left(\Delta P_i - |\Delta P_i| \right), \tag{A.13}$$

where Eq. (A.12) states that the battery can only charge if there is excess solar power available (P_{avail}). Eq. (A.13) states that the battery must

Table A.1
Experimental Setup Details.

	Irbid, Jordan		Agadir, Morocco	
	Controller Field	Reference Field	Controller Field	Reference Field
Valve Operation	Manual	Manual	Automatic	Manual
Irrigation scheduling	POWEIr optimization	Local farmer recommendation	POWEIr optimization	Local farmer
Electricity	Solar	Grid	Solar	Solar
Farm Type	Half of research station	Half of research station	Research station	Small farm, sells at local market
Crops	Okra + Grape	Okra + Grape	Potato; Carrot	Potato; Carrot
Experiment time frame	March-Dec 2023	March-Dec 2023	Feb-June, 2023; July-No. 2023	Feb-June, 2023; July-No. 2023
Soil Texture	Loam, Sandy Clay	Loam, Sandy Clay	Sandy Loam	Sandy Loam
Field Size	0.5 ha, each crop	0.5 ha, each crop	0.6 ha	0.6 ha
Number of Sections	6	6	6	4

Table A.2
Parameter inputs for POWEIr controller experiments and yield loss simulation.

Input	Units	Jordan		Morocco	
Crop	–	Grape	Okra	Potato	Carrot
Field area	ha	0.5	0.5	0.6	0.6, 3 (virtual)
Season	–	May-Dec 2023		Jan-Jun 2023	July-No. 2023
Soil texture	–	Loam and Sandy Clay		Sandy Loam	
$K_{c\ [ini,mid,late]}$	–	[0.3, 0.7, 0.54]	[0.46, 1.03, 0.7]	[0.4, 0.96, 0.68]	[0.6, 1, 0.9]
$Z_{r\ [min,max]}$	–	[0.4, 1.1]	[0.2, 0.9]	[0.2, 0.63]	[0.1, 0.65]
$K_{y\ [ini,dev,mid,late]}$	–	[0.2, 0.7, 0.85, 0.4]	1.25	[0.6, 1.5, 0.7, 0.2]	[0.2, 0.95, 0.45, 0.6]
k_{RO}	–	0.5 (loam), 0.375 (sandy clay)		0.25	
A_s	m^2	[1980, 1764, 1665, 1512, 1728, 1296]	[1980, 1764, 1665, 1512, 3024]	920	
f_w	–	0.1	0.36	0.3	0.51
$TAW_{[min,max]}$	mm	[52, 145]	[26, 119]	[24, 76]	[12, 78]
$f_{d,const}$	–	0.35	0.3	0.35	0.35
Y_{max}	kg/ha	7196	13,559	5948	6305
k_b	USD/kWh	303		711	
u_{max}	kW	13.8		12.4	
k_w	USD/m^3	0.001			
q_s	m^3/h	[5.1, 5.4, 4.5, 4.5, 4.98, 4.98]	[8.4, 8.4, 7.2, 8.4, 15.6]	8.7	
k_c	USD/kg	0.866	1.726	0.244	0.228
k_d	USD/day	0.847		0.929	
ρ_{soil}	g/cm^3	1.4 (loam), 1.1 (sandy clay)		1.29	

discharge to meet the pump power demand, P_{pump} (kW), if there is insufficient solar power available, P_{avail} (kW). The battery efficiency, η_{batt}, is assumed to be the same for charging and discharging. P_{pump} is an empirical linear equation fit as a function of the number of sections opened at a given time; these values are calibrated when a system is installed. The constraints on section opening are

$$\sum_{s} d_{s,i} \leq d_{max}, \tag{A.14}$$

$$\sum_{i}^{N_{day}} (d_{s,i} - d_{s,i-1})^2 \leq 2, \tag{A.15}$$

where $d_{\max}$, a user-specified constant, is the maximum number of sections that can be opened at one time. Eq. (A.15) requires each section to be opened and closed only once per day at most. Eq. (A.15) prevents the optimization from generating a schedule that requires the user to open and close a section multiple times within a single day to avoid unnecessary labor.

A.2. Controller experiment and simulation inputs

The experimental setup details are shown in Table A.1. The inputs to the POWEIr controller used in the experiment are shown in Table A.2.

A.3. Supplementary experiment results

The cumulative pump energy broken down into hydraulic pump output energy, calculated input pump power, and measured input power to the pump for the farm with the controller and the reference farm are shown in Fig. A.1 for the Morocco carrot season. Fig. A.2 shows the pump efficiency at the farm with the controller and the reference farm for the Morocco carrot season.

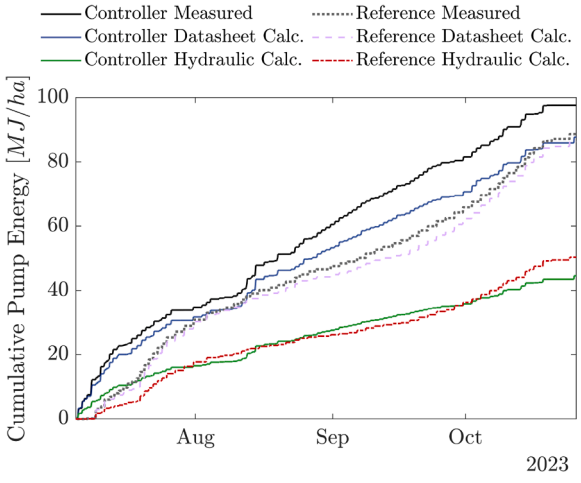

Fig. A.1. Cumulative pumping energy breakdown comparison between the farm with the POWEIr controller and the reference farm for the Morocco carrot season. The 'Hydraulic Pump' energy was calculated from the flow and pressure at the pump. The 'Pump Datasheet' energy was calculated by dividing the 'Hydraulic Pump' by the pump efficiency, with pump efficiency calculated from the measured flow rate according to the pump's efficiency curve reported by the manufacturer.

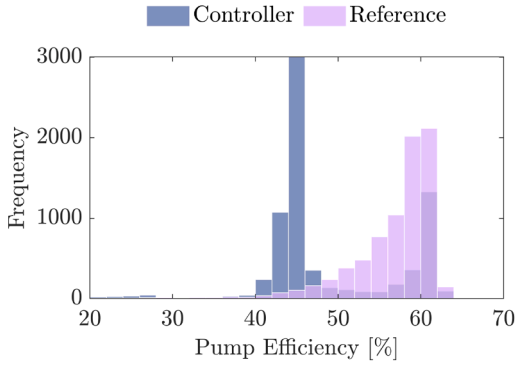

Fig. A.2. Histogram of the pump efficiency for the farm with the POWEIr controller and reference farm for the Morocco carrot season. The pump efficiency was calculated at all irrigation times from the measured flow rate according to the pump's efficiency curve reported by the manufacturer.

References

[1] UN, The Sustainable Development Goals Report 2023: Special Edition, United Nations Department of Economic and Social Affairs, 2023.

[2] U. Khanal, C. Wilson, S. Rahman, B.L. Lee, V.-N. Hoang, Smallholder farmers' adaptation to climate change and its potential contribution to UN's sustainable development goals of zero hunger and no poverty, J. Clean. Prod. 281 (2021) 124999.

[3] J.D. Sachs, G. Schmidt-Traub, M. Mazzucato, D. Messner, N. Nakicenovic, J. Rockström, Six transformations to achieve the sustainable development goals, Nat. Sustain. 2 (9) (2019) 805–814.

[4] United Nations Global Sustainable Development Goal (SDG) Indicators Data Platform, (2023), (https://unstats.un.org/sdgs/dataportal). [Accessed: 2023-09-30].

[5] Food and Agriculture Organization of the United Nations Data Platform, (2010), (https://www.fao.org/faostat). [Accessed: 2010-09-30].

[6] M. Crippa, E. Solazzo, D. Guizzardi, F. Monforti-Ferrario, F.N. Tubiello, A. Leip, Food systems are responsible for a third of global anthropogenic GHG emissions, Nat. Food 2 (3) (2021) 198–209.

[7] B. Paris, F. Vandorou, A.T. Balafoutis, K. Vaiopoulos, G. Kyriakarakos, D. Manolakos, G. Papadakis, Energy use in open-field agriculture in the EU: a critical review recommending energy efficiency measures and renewable energy sources adoption, Renew. Sustain. Energy Rev. 158 (2022) 112098.

[8] W. Bank, Beyond Scarcity: Water Security in the Middle East and North Africa, MENA Development Report; World Bank, 2018. https://doi.org/10.1596/978-1-4648-1144-9

[9] IRENA and FAO, Renewable Energy for Agri-Food Systems – Towards the Sustainable Development Goals and the Paris agreement, Abu Dhabi and Rome, 2021. https://doi.org/10.4060/cb7433en

[10] S. Balasubramanya, D. Garrick, N. Brozović, C. Ringler, E. Zaveri, A.-S. Rodella, M.-C. Buisson, P. Schmitter, N. Durga, A. Kishore, T.T. Minh, K. Kafle, D. Stifel, S. Balasubramanya, A. Chandra, L. Hope, Risks from solar-powered groundwater irrigation, Science 383 (2024) 256–258. https://doi.org/10.1126/science.adi9497

[11] GeoFactbook: World Facts and Statistics, "Irrigated Land 2025", 2026, (https://geofactbook.com/fact/irrigated-land/2025). [Accessed 31-03-2026].

[12] A. Dutta, Solar promises in parched fields: is PM-KUSUM India's quiet agricultural revolution (2026). [Accessed 31-03-2026].

[13] India Ministry of New and Renewable Energy, "PM-KUSUM Benefits Reach Over 21.77 Lakh Farmers Across the Country", 2026, (Press releas https://www.pib.gov.in/PressReleasePage.aspx?PRID=2244667&reg=3&lang=2). [Accessed 31-03-2026].

[14] J. Jägermeyr, D. Gerten, J. Heinke, S. Schaphoff, M. Kummu, W. Lucht, Water savings potentials of irrigation systems: global simulation of processes and linkages, Hydrol. Earth Syst. Sci. 19 (7) (2015) 3073–3091.

[15] P. Yang, L. Wu, M. Cheng, J. Fan, S. Li, H. Wang, L. Qian, Review on drip irrigation: impact on crop yield, quality, and water productivity in China, Water 15 (9) (2023) 1733.

[16] G.D. Van de Zande, F. Grant, C. Sheline, S. Amrose, J. Costello, A. Ghodgaonkar, A.G. Winter V, Design and evaluation of a precision irrigation tool's human-machine interaction to bring water-and energy-efficient irrigation to resource-constrained farmers, Sustainability 16 (19) (2024) 8402.

[17] U. Daraz, Š. Bojnec, Y. Khan, Energy-efficient smart irrigation technologies: a pathway to water and energy sustainability in agriculture, Agriculture 15 (5) (2025) 554. https://doi.org/10.3390/agriculture15050554

[18] C. Sheline, F. Grant, S. Gelmini, S. Pratt, A.G. Winter V, Designing a predictive optimal water and energy irrigation (POWEIr) controller for solar-powered drip irrigation systems in resource-constrained contexts, Appl. Energy (2024). https://doi.org/10.1016/j.apenergy.2024.124107

[19] G. Todde, M. Caria, A. Pazzona, L. Ledda, L. Narvarte, Does precision photovoltaic irrigation represent a sustainable alternative to traditional systems?, in: Innovative Biosystems Engineering for Sustainable Agriculture, Forestry and Food Production, Springer International Publishing, 2020, pp. 585–593. https://doi.org/10.1007/978-3-030-39299-4_64

[20] A. Merida Garcia, I. Fernandez Garcia, E. Camacho Poyato, P. Montesinos Barrios, J.A. Rodriguez Diaz, Coupling irrigation scheduling with solar energy production in a smart irrigation management system, J. Clean. Prod. 175 (2018) 670–682.

[21] N. Durga, P. Schmitter, C. Ringler, S. Mishra, M.S. Magombeyi, A. Ofosu, P. Pavelic, F. Hagos, D. Melaku, S. Verma, T. Minh, C. Matambo, Barriers to the uptake of solar-powered irrigation by smallholder farmers in sub-saharan Africa: a review, Energy Strategy Rev. 51 (2024). https://doi.org/10.1016/j.esr.2024.101294

[22] V.K. Hebsale Mallappa, R. Bansal, Economic feasibility and farmers' willingness to adopt solar-powered irrigation pumps (SPIPs) for self-reliance, Energy Strategy Rev. 64 (2026). https://doi.org/10.1016/j.esr.2026.102094

[23] Nurmalitasari, Nurchim, R.D. Lestari, Artificial intelligence-driven solar smart irrigation for sustainable agriculture: trends, challenges, and SDG implications - A systematic review, Smart Agric. Technol. 12 (2025) 101665. https://doi.org/10.1016/j.atech.2025.101665

[24] G. Jobbins, J. Kalpakian, A. Chriyaa, A. Legrouri, E.H. El Mzouri, To what end? Drip irrigation and the water-energy-food nexus in Morocco, Int. J. Water Resour. Dev. 31 (3) (2015) 393–406.

[25] F.A. Ward, M. Pulido-Velazquez, Water conservation in irrigation can increase water use, Proc. Natl. Acad. Sci. 105 (47) (2008) 18215–18220.

[26] M. Benouniche, M. Kuper, A. Hammani, H. Boesveld, Making the user visible: analysing irrigation practices and farmers' logic to explain actual drip irrigation performance, Irrig. Sci. 32 (2014) 405–420.

[27] E. Bwambale, F.K. Abagale, G.K. Anornu, Smart irrigation monitoring and control strategies for improving water use efficiency in precision agriculture: a review, Agric. Water Manag. 260 (2022) 107324.

[28] G.D. Van de Zande, C. Sheline, A.G. Winter, Evaluating the potential for a novel irrigation system controller to be adopted by medium-scale contract farmers in East Africa, in: Volume 6: 34th International Conference on Design Theory and Methodology (DTM), American Society of Mechanical Engineers, St. Louis, Missouri, USA, 2022, V006T06A037.

[29] E.A. Abioye, M.S.Z. Abidin, M.S.A. Mahmud, S. Buyamin, M.H.I. Ishak, M.K. I.A. Rahman, A.O. Otuoze, P. Onotu, M.S.A. Ramli, A review on monitoring and advanced control strategies for precision irrigation, Comput. Electron. Agric. 173 (2020) 105441.

[30] A. Sarr, A.K. Chandel, L. Diop, Y.M. Soro, A.K. Tossa, S. Hota, A. Manimozhian, Agroclimatic sensing, communication, and computational systems-based methods and technologies for precision irrigation management: current state and prospects, Computers 15 (2) (2026) 137. https://doi.org/10.3390/computers15020137

[31] FAO, The state of food and agriculture 2022, Leveraging Automation in Agriculture for Transforming Agrifood Systems, Rome, FAO, 2022.

[32] S.K. Kasereka, T. Tashev, Y.-C.N. Medagbe, O.V. Ocama, G.W.K. Ilunga, E. Kyungu, K. Kyamakya, Smart irrigation for precision agriculture: a pathway to sustainable farming in low-income regions, in: 2025 International Conference on Big Data, Knowledge and Control Systems Engineering (BdKCSE), IEEE, 2025, p. 1–9. https://doi.org/10.1109/bdkcse67969.2025.11300531

[33] J. Bayar, N. Ali, Z. Cao, Y. Ren, Y. Dong, Artificial intelligence of things (AIoT) for precision agriculture: applications in smart irrigation, nutrient and disease management, Smart Agric. Technol. 12 (2025) 101629. https://doi.org/10.1016/j.atech.2025.101629

[34] E. Bwambale, J. Wanyama, T.A. Adongo, E. Umukiza, R. Ntole, S.R. Chikavumbwa, D. Sibale, Z. Jeremaih, A review of model predictive control in precision agriculture, Smart Agric. Technol. 10 (2025) 100716. https://doi.org/10.1016/j.atech.2024.100716

[35] C. Sheline, S. Ingersoll, S. Amrose, S. Irmak, A.G. Winter V, Sensitivity study of the predictive optimal water and energy irrigation (POWEIr) controller's schedules for sustainable agriculture systems in resource-constrained contexts, Comput. Electron. Agric. (2024). https://doi.org/10.1016/j.compag.2024.109230

[36] E.A. Abioye, M.S.Z. Abidin, M.N. Aman, M.S.A. Mahmud, S. Buyamin, A model predictive controller for precision irrigation using discrete lagurre networks, Comput. Electron. Agric. 181 (2021) 105953.

[37] Y. Ding, L. Wang, Y. Li, D. Li, Model predictive control and its application in agriculture: a review, Comput. Electron. Agric. 151 (2018) 104–117.

[38] D. Delgoda, H. Malano, S.K. Saleem, M.N. Halgamuge, Irrigation control based on model predictive control (MPC): formulation of theory and validation using weather forecast data and AQUACROP model, Environ. Model. Softw. 78 (2016) 40–53.

[39] E. Bwambale, F.K. Abagale, G.K. Anornu, Towards a modelling, optimization and predictive control framework for smart irrigation, Heliyon 10 (18) (2024) e38095. https://doi.org/10.1016/j.heliyon.2024.e38095

[40] A. Liu, D. Zhao, Y. Wei, Model predictive control of adaptive irrigation decisions incorporating rainfall intensity and soil properties, Agriculture 15 (5) (2025) 527. https://doi.org/10.3390/agriculture15050527

[41] C. Lozoya, C. Mendoza, A. Aguilar, A. RomÃ¡n, R. CastellÃ³, et al., Sensor-based model driven control strategy for precision irrigation, J. Sens. 2016 (2016) 1–12.

[42] I. Fernández García, J.A. Rodríguez Díaz, E. Camacho Poyato, P. Montesinos, Optimal operation of pressurized irrigation networks with several supply sources, Water Resour. Manag. 27 (8) (2013) 2855–2869.

[43] J.M. Navarro Navajas, P. Montesinos, E.C. Poyato, J.A. Rodríguez Díaz, Impacts of irrigation network sectoring as an energy saving measure on olive grove production, J. Environ. Manag. 111 (2012) 1–9.

[44] S. Robertson, J. Robertson, "Mastering the Requirements Process: Getting Requirements Right", Addison-Wesley Educational, 3, 2012.

[45] K.T. Ulrich, S.D. Eppinger, M.C. Yang, Product Design and Development, McGraw-Hill Education, New York, NY, seventh edition, 2020.
[46] National Water Strategy 2023–2040, The Ministry of Water and Irrigation, Jordan, 2023.
[47] Generation Green 2020–2030, Ministry of Agriculture, Fisheries, Rural Development, Water, and Forests: Department of Agriculture, Morocco, 2020.
[48] G.D. Van de Zande, C. Sheline, S. Pratt, V. Winter, Amos G., Water savings and user-centered validation of an automatic scheduling-manual operation (AS-MO) irrigation tool: a case study on a Jordanian farm, in: Proceedings of the International Design Engineering Technical Conferences and Computers and Information in Engineering Conference, Volume 3B: 50th Design Automation Conference (DAC), ASME, Washington, DC, USA, 2024, V03BT03A019. https://doi.org/10.1115/DETC2024-142549
[49] R. Alley, K. Emanuel, F. Zhang, Advances in weather prediction, Science 363 (2019) 342–344.
[50] E. Nkiaka, A. Taylor, A. Dougill, Identifying user needs for weather and climate services to enhance resilience to climate shocks in sub-Saharan Africa, Environ. Res. Lett. 14 (2019) 123003.
[51] G. Brunet, D.B. Parsons, D. Ivanov, B. Lee, P. Bauer, N.B. Bernier, V. Bouchet, A. Brown, A. Busalacchi, G.C. Flatter, et al., Advancing weather and climate forecasting for our changing world, Bull. Am. Meteorol. Soc. 104 (4) (2023) E909–E927.
[52] D.P. Rogers, V.V. Tsirkunov, H. Kootval, A. Soares, D. Kull, A.-M. Bogdanova, M. Suwa, Weathering the Change: How to Improve Hydromet Services in Developing Countries?, World Bank, 2019.
[53] C. Sheline, V. Winter, Amos, Machine learning method for forecasting weather needed for crop water demand estimations in low-resource settings using a case study in Morocco, 3B: 47th Design Automation Conference (DAC), American Society of Mechanical Engineers, 2021. https://doi.org/10.1115/DETC2021-70571
[54] R.G. Allen, L.S. Pereira, D. Raes, M. Smith, Crop evapotranspiration: guidlines for computing crop water requirements, FAO Irrigation and Drainage Paper No. 56 (1998).
[55] P. Steduto, T.C. Hsiao, E. Fereres, D. Raes, Crop yield response to water, FAO Irrigation and Drainage Paper No. 66 (2012).
[56] J. Doorenbos, A.H. Kassam, Yield response to water, FAO Irrigation and Drainage Paper No. 33 (1979).
[57] J.W. Bishop, Computer simulation of the effects of electrical mismatches in photovoltaic cell interconnection circuits, Sol. Cells 25 (1988) 73–89.
[58] W. De Soto, S.A. Klein, W.A. Beckman, Improvement and validation of a model for photovoltaic array performance, Sol. Energy 80 (1) (2006) 78–88.
[59] S. Gautam, Time Series Forecasting of Solar Radiation, 2021, (https://towardsdatascience.com/time-series-forecasting-of-solar-radiation-294b2a0c94e5). [Accessed: 2021-12-01].
[60] M. Gao, J. Li, F. Hong, D. Long, Day-ahead power forecasting in a large-scale photovoltaic plant based on weather classification using LSTM, Energy 187 (2019) 115838.
[61] X. Qing, Y. Niu, Hourly day-ahead solar irradiance prediction using weather forecasts by LSTM, Energy 148 (2018) 461–468.
[62] Keras, 2021, (https://keras.io/). [Accessed: 2021-11-30].
[63] D.P. Kingma, J. Ba, Adam: a method for stochastic optimization, (2014). arXiv:1412.6980
[64] J. Sokol, J. Narain, J. Costello, T. McLaurin, D. Kumar, A.G. Winter, Analytical model for predicting activation pressure and flow rate of pressure-compensating inline drip emitters and its use in low-pressure emitter design, Irrig. Sci. 40 (2) (2022) 217–237.
[65] F. Grant, C. Sheline, J. Sokol, S. Amrose, E. Brownell, V. Nangia, A.G. Winter, Creating a solar-powered drip irrigation optimal performance model (SDrOP) to lower the cost of drip irrigation systems for smallholder farmers, Appl. Energy 323 (2022) 119563.
[66] F. Grant, C. Sheline, S. Amrose, E. Brownell, V. Nangia, S. Talozi, A. Winter, Validation of an analytical model to lower the cost of solar-powered drip irrigation systems for smallholder farmers in the MENA region, in: Volume 11B: 46th Design Automation Conference (DAC), American Society of Mechanical Engineers, 2020. https://doi.org/10.1115/detc2020-22610
[67] F. Grant, Product Architectures for Solar-Powered Drip Irrigation (SPDI) Systems in the Middle East and North Africa, Ph.D. thesis, Massachusetts Institute of Technology, 2025.
[68] L.E. Williams, Irrigation Scheduling: Use of Reference ET (ETo) and Crop Coefficients (Kc), 2019, (UC Davis Viticulture and Enology, Kearney Agricultural Research and Extension Center). Workshop presentation, https://wineserver.ucdavis.edu/sites/g/files/dgvnsk2676/files/inline-files/1%20LEW%20Irrigation%20Shortcourse%20Napa%202019.pdf.
[69] A. Unlukara, B. Cemek, Response of okra to water stress, Mustafa Kemal "Univ. Tar/Bilim. Derg. 24 (2019) 313–319.
[70] S. Ayas, Response of okra (Abelmoschus Esculentus l. Yalova Akköy-41) to different irrigation and fertigation levels, Turk. J. Agric.-Food Sci. Technol. 8 (10) (2020) 2225–2235.
[71] C.S. Patil, Crop coefficient and water requirement of Okra (Abelmoschus Esculentus L. Moench), Mausam 61 (1) (2010) 121–124.
[72] R. Folea, Click PLC: Temperature PID Tuning Resource Page, 2021. https://library.automationdirect.com/click-plc-temperature-pid-tuning-resource-page/
[73] System Identification: Identify Models of Dynamic Systems From Measured Data - MATLAB, 2026. https://www.mathworks.com/help/ident/ref/systemidentification-app.html?s_tid=srchtitle_site_search_1_systemidentification
[74] G.F. Franklin, J.D. Powell, A. Emami-Naeini, Feedback Control of Dynamic Systems, Pearson, Upper Saddle River, NJ, 7 edition, 2014.
[75] L. Zotarelli, M.D. Dukes, M. Paranhos, Minimum number of soil moisture sensors for monitoring and irrigation purposes, Edis 2013 (7) (2013) HS1222.
[76] R.S. Ayers, D.W. Westcot, et al., Water Quality for Agriculture, vol. 29, Food and Agriculture Organization of the United Nations Rome, 1985.
[77] B. Anita, N. Selvaraj, Biology, yield loss and integrated management of root-knot nematode, Meloidogyne hapla infecting carrot in Nilgiris, Indian J. Nematol. 41 (2) (2011) 144–149.
[78] S.A. Anwar, M.V. McKenry, Incidence and population density of plant-parasitic nematodes infecting vegetable crops and associated yield losses in Punjab, Pakistan, Pak. J. Zool. 44 (2) (2012).
[79] R.M. Davis, J. Nuñez, Integrated approaches for carrot pests and diseases management, in: General Concepts in Integrated Pest and Disease Management, Springer, 2007, pp. 149–188.
[80] R. Singh, U. Kumar, Assessment of nematode distribution and yield losses in vegetable crops of Western Uttar Pradesh in India, Int. J. Sci. Res. 4 (5) (2015) 2812–2816.
[81] T.L. Widmer, J.W. Ludwig, G.S. Abawi, The northern root-knot nematode on carrot, lettuce, and onion in New York, Technical Report, New York State Agricultural Experiment Station, 1999.
[82] K.X. Soulis, S. Elmaloglou, N. Dercas, Investigating the effects of soil moisture sensors positioning and accuracy on soil moisture based drip irrigation scheduling systems, Agric. Water Manag. 148 (2015) 258–268.
[83] S. Touil, A. Richa, M. Fizir, J.E. Argente García, A.F. Skarmeta Gómez, A review on smart irrigation management strategies and their effect on water savings and crop yield, Irrig. Drain. (2022). https://doi.org/10.1002/ird.2735
[84] OpenJS Foundation and Contributors Node-RED [Online] (2023) Available:https://nodered.org
[85] Influx Data Inc InfluxDB (2023) [Online]. Available: https://www.influxdata.com/